

39 mild brittle deformation with rare faults, characterized by small displacement, and
40 widespread extension joints, frequently organized in sets. Therefore, we conducted a
41 quantitative and systematic analysis of the joint sets affecting Quaternary deposits, by
42 applying an inversion technique *ad hoc* to infer the orientation and ratio of the principal
43 stress axes, $R = (\sigma_2 - \sigma_3)/(\sigma_1 - \sigma_3)$. Within a general extensional regime, we recognized
44 three deformational events of regional significance. The oldest event, constrained to the
45 early and middle part of the Middle Pleistocene, is characterized by variable direction of
46 extension and R between 0.64-0.99. The penultimate event, dated late Middle
47 Pleistocene, is characterized by an almost uniaxial tension, with a horizontal σ_3 striking
48 \sim N43°E; R is high, between 0.85-0.99. The most recent event is characterized by the
49 lowermost R values, that never exceed 0.47 and are frequently <0.30 , indicating a sort
50 of horizontal ‘radial’ extension. This event is not older than the Late Pleistocene and
51 possibly reflects the active stress field still dominating the entire study area.

52

53

54

55 **Keywords:** Quaternary tectonics, brittle deformation, fracture, Pleistocene

56

57

58 **1. Introduction**

59

60 The foreland of the Apennines fold-and-thrust belt (Italy) corresponds essentially to the
61 Adriatic Sea (Fig. 1), that has long been considered a tectonically and seismically
62 “stable” area. Only in its central sector, this foreland is characterized by significant
63 historical and instrumental seismicity (Gruppo di Lavoro CPTI, 2004; Castello et al.,
64 2005; Fig. 2), both off-shore (active Mesoadriatic strip; Console et al., 1993) and on-
65 land (Molise-Gondola shear zone; Di Bucci et al., 2006; Fig. 1), and some seismogenic
66 faults have already been identified (DISS Working Group, 2007, and references therein;
67 Di Bucci et al., 2009b).

68 This foreland is exposed on-land only in the easternmost sector of the Italian
69 peninsula, i.e. in the Apulia region (Fig. 1). Northern Apulia is the locus of rare but
70 destructive historical earthquakes (Gruppo di Lavoro CPTI, 2004), occasionally
71 associated with surface faulting (Piccardi, 2005) and possibly with coseismic uplift of
72 limited parts of the coastal area (Mastronuzzi and Sansò, 2002a). The Tyrrhenian (MIS
73 5.5, ~125 ka) coastline is variously displaced from the Ionian side to the Adriatic one,
74 indicating inhomogeneous tectonic behaviour during the Late Pleistocene (e.g. Bordoni
75 and Valensise, 1998; Ferranti et al., 2006). Seismites have been recognized in Upper
76 Pleistocene deposits along the southern Adriatic coasts, testifying to the occurrence of
77 strong ground shaking, that has been associated with Late Pleistocene earthquakes
78 located within a ~40 km distance from the seismites outcrops (Tropeano et al., 1997;
79 Fig. 3). In contrast, only one moderate historical earthquake occurred in Southern
80 Apulia (1826 Manduria earthquake, I_{max} =VI-VII, $M=5.3$; Gruppo di Lavoro CPTI,
81 2004; Fig. 2). Indeed, in 1743 the southern portion of the Adriatic foreland was hit by a
82 severe earthquake sequence (which also triggered a tsunami; Mastronuzzi and Sansò,

83 2004; Tinti et al., 2004; Mastronuzzi et al., 2007a), but these events have been
84 positively located off-shore ($I_{max}=IX-X$, $M=6.9$; Gruppo di Lavoro CPTI, 2004;
85 Guidoboni and Ferrari, 2004).

86 On the one hand, this brief overview can explain why the active geodynamics of
87 the Adriatic block is still debated. In the lack of a shared interpretation, different models
88 have been proposed, among which the buckling of a thick continental lithosphere, either
89 within an active subduction beneath the Southern Apennines or due to horizontal
90 compression, or the NW-SE Eurasia-Nubia convergence. On the other hand, this
91 overview also suggests that Southern Apulia, a region whose recent deformation was
92 never investigated from a mesostructural point of view, is in need of a detailed analysis
93 that may help to outline its recent tectonic evolution and its present-day deformation
94 regime. Preliminary results of an original structural analysis carried out with this
95 purpose indicate that Middle and Late Pleistocene deposits in Southern Apulia have
96 been affected by mild but recurrent and discernible brittle deformation (Di Bucci et al.,
97 2009a). Faults are rare and all characterized by small displacement values, whereas
98 extension joints prevail in most of the investigated sites, they are frequently well
99 exposed and organized in sets. The occurrence of this mild tectonic deformation, and
100 the lack of a significant number of shear planes (even of faults at the mesoscale)
101 affecting Quaternary deposits, led us to approach the identification of the causative
102 stress field by an in-depth quantitative analysis of the joint sets and of their relationships
103 with one another. Here we present the results of this innovative approach, which was
104 never attempted before for the characterization of the active deformation of the southern
105 Adriatic foreland.

106

107 **2. Geology of Apulia**

108

109 *2.1. Tectonic outline*

110

111 The Adriatic foreland is shared among key fold-and-thrust belts of the Central
112 Mediterranean, i.e., the Albanides, the Dinarides, and the Apennines of peninsular Italy.
113 Apennines are a Late Cenozoic-Quaternary accretionary wedge, which forms part of the
114 Africa-verging mountain system in the Alpine-Mediterranean area. In the Southern
115 Apennines, this wedge is formed by east-to-northeast verging thrust sheets deriving
116 from palaeogeographic domains of alternating carbonate platforms and pelagic basins
117 (e.g. Mostardini and Merlini, 1986; Patacca and Scandone, 1989; Fig. 1). The most
118 external of these domains is the Apulia Platform, a ~6 km-thick succession of neritic
119 Mesozoic carbonate rocks (Ricchetti, 1980). This succession is partially overlain by
120 mainly terrigenous marine deposits of Cenozoic age (Patacca and Scandone, 2004; Figs.
121 1 and 3).

122 The Apulia Platform and its underlying basement are partly involved in the
123 orogenic wedge (Menardi Noguera and Rea, 2000; Butler et al., 2004), partly form the
124 foreland inflected below the outer front of the Apennines (Mostardini and Merlini,
125 1986), and partly form the Adriatic foreland *sensu stricto*, both on-land and off-shore
126 (Gargano, Central Apulia, Salento and Southern Adriatic Sea; Fig. 1). Southern
127 Apennines migrated toward the Adriatic foreland up to the beginning of the Middle
128 Pleistocene, when the motion of the wedge front is reported to have ceased (Patacca and
129 Scandone, 2004). Meanwhile, SW-NE-trending extension, already affecting the inner
130 part of the belt (Papanikolaou and Roberts, 2007, among many others), became
131 dominant over the core of the Apennines, probably as a result of a geodynamic change

132 that took place around 800 ka (e.g. Cinque et al., 1993; Hippolyte et al., 1994). This
133 tectonic regime is still active, as demonstrated by breakout and seismicity data
134 (Montone et al., 2004), and accounts for large earthquakes generated by NW-SE–
135 striking normal faults straddling the topographic divide of the Southern Apennines
136 (Gruppo di Lavoro CPTI, 2004; DISS Working Group, 2007, with references; Fig. 2).
137 In contrast, recent instrumental evidence shows that to the northeast of the Apennines
138 ridge the SW-NE extension is associated with NW-SE horizontal compression
139 (Vannucci and Gasperini, 2004; Boncio et al., 2007; Del Gaudio et al., 2005; 2007). For
140 instance, the 2002 Molise earthquakes (Figs. 1 and 2) supplied living evidence that, in
141 the frontal part of the chain, large upper crustal NW-SE normal faults give way to
142 deeper E-W, right-lateral, seismogenic faults (Borre et al., 2003; Di Luccio et al., 2005).
143 Major E-W–oriented shear zones have been described in literature roughly between the
144 latitudes 40°30'N and 42°30'N, both on-land and off-shore (Di Bucci and Mazzoli,
145 2003; Valensise et al., 2004; both with references). They extend for tens of kilometres
146 below the outer front of the Southern Apennines orogenic wedge and, toward the east,
147 below the foredeep deposits up to the foreland. Their present-day activity is interpreted
148 as due to the reactivation of inherited zones of weakness. Among them, the best
149 constrained is referred to as Molise-Gondola shear zone, that has a clear geologic and
150 seismogenic signature (MGsz; Di Bucci et al., 2006, with references; Fig. 1). Further
151 south, another regional E-W lineament extending between Potenza and Taranto has
152 been recently interpreted as active and seismogenic (DISS Working Group, 2007), as it
153 includes the source area of a series of M5+ earthquakes that were caused by right-lateral
154 slip on E-W planes at 15-23 km depth (1990-1991 Potenza earthquakes; Boncio et al.,
155 2007, with references; Fig. 2).

156 Assessing whether the southernmost portion of Apulia is tectonically active is
157 made more difficult by the following circumstances: (1) seismicity is low, widespread
158 and seemingly trendless; (2) no information on the active stress field is available from
159 breakout data; (3) geomorphological studies indicate that the southernmost tip of the
160 study area underwent uplift during the Middle Pleistocene, followed by a relative
161 stability during the past 330 ka (Mastronuzzi et al., 2007b), while the Taranto area has
162 been uplifted at 0.14-0.25 mm/a since the Late Pleistocene (Bordoni and Valensise,
163 1998; Ferranti et al., 2006; Caputo et al., 2007).

164

165 *2.2. Quaternary setting*

166

167 Although considered as a stable area, the Apulia portion of the Adriatic foreland shows
168 geological evidence for the interplay between the build-up of the Apennines and
169 Dinarides chains and the eustatic sea level changes in Pleistocene times. Therefore, the
170 detailed analysis of the Southern Murge Plateau and Salento Peninsula provides a more
171 complex Quaternary evolution, marked by alternating phases of sea transgression and
172 continentality, that are controlled in part by the tectonic activity.

173

174 Bradanic foredeep cycle. During the Late Pliocene-Middle Pleistocene, Apulia was
175 marked by relative sea level stages higher than the present one. During this time interval
176 the foredeep area, submerged by the paleo-Adriatic Sea, was characterized by the
177 deposition of bioclastic calcarenites (Calcareniti di Gravina Fm; e.g., Iannone and Pieri,
178 1979; D'Alessandro and Iannone, 1982; 1984; Tropeano et al., 2002 and references
179 therein; Fig. 4), giving way to grey-bluish clayey marls toward the Taranto Gulf
180 (Argille subappennine Fm; e.g., Marino, 1996; Ciaranfi et al., 2001; Maiorano et al.,

181 2008, and references therein). This sedimentary event is closed by coarse terrigenous
182 deposits.

183 There is partial agreement concerning the interpretation and chronological
184 attribution of the Lower-Middle Pleistocene deposits that crop out in the Salento
185 Peninsula. In this lapse of time, almost the entire Salento was under sub-aerial
186 conditions but its southeasternmost part. Here, bioclastic massive calcarenites heteropic
187 to gray-bluish silty clays have been referred exclusively to the latest Early Pleistocene
188 by Bossio et al. (1991, and references therein). On the contrary, other investigators refer
189 to the Pliocene-Lower Pleistocene stratigraphic interval the deposits which crop out in
190 Salento (Tropeano et al., 2004).

191 A considerable number of studies is available for the Bradanic foredeep (Ciaranfi
192 et al., 2001; Maiorano et al., 2008 and references therein), whereas very few data have
193 been collected on the silty-clay deposits frequently exposed along the coast between
194 Brindisi and Lecce, or near Taranto (i.e., Ricchetti, 1967; 1972; Fig. 3), at the bottom of
195 the Marine Terraced Deposits (see next subsection). In the former zone, Coppa et al.
196 (2001) dated to the Early-Middle Pleistocene a succession exposed along the Torre San
197 Gennaro cliff. In the latter zone, the age of an ash layer interlayered in the silty clay
198 constrains its deposition at ~1.2 Ma (Capaldi et al., 1979). In the Cheradi Islands, in
199 front of the Taranto harbour, new data from nannoplancton analyses on a silty-sand
200 deposit suggest a Middle Pleistocene age, based on the presence of *Gephyrocapsa* sp3
201 (Mastronuzzi and Sansò, 1998).

202

203 Marine Terraced Deposits. Up to 15-20 m thick, bioclastic, sandy-calcarenitic
204 sediments, the so-called Marine Terraced Deposits, crop out all around the Murge
205 Plateau and in Salento up to an elevation of 300-400 m and are dated Middle-Upper

206 Pleistocene (Ciaranfi et al., 1988; Fig. 4). Marine sediments are frequently associated
207 with well-cemented aeolian deposits, arranged in a continuous dune belt. These covers
208 formed during repeated marine transgressions, which probably affected only in part, or
209 even never, the eastern and southern part of Salento (Mastronuzzi et al., 2007b).

210 The best known among the Marine Terraced Deposits are those along the coast
211 stretching from Taranto to Gallipoli, referred to the latest Middle Pleistocene and/or to
212 the Last Interglacial Period (e.g. Hearty and Dai Pra, 1992; Belluomini et al., 2002 and
213 references therein), as well as those belonging to the Middle-Upper Pleistocene
214 succession recognized between Gallipoli and Leuca (D'Alessandro and Massari, 1997).
215 On the contrary, several outcrops in other parts of Salento are still poorly studied.

216 Middle-Upper Pleistocene deposits can be found also in the inner parts of the
217 study area (D'Alessandro et al., 1994). The complete sedimentary succession, from
218 bottom to top, is formed by massive yellow-greenish clayey sands, very rich in
219 glauconite, called "Sabbie a Brachiopodi" (sands with Brachiopods). The related
220 paleontological assemblage is marked by the presence of *Terebratula scillae* Seguenza
221 and suggests a deposition depth >100 m (D'Alessandro and Palmentola, 1978;
222 D'Alessandro et al., 1994). The Sabbie a Brachiopodi are covered by silty clays of
223 shallower marine environment (Salvatorini 1969; D'Alessandro et al., 1994). An
224 erosional surface separates the top of these deposits from a sandy silt rich in quartz,
225 micas, carbonate rock fragments and scarce oligotypic fauna (mainly *Clamys* sp. and
226 *Ostrea* sp.). Fauna content and sedimentological observations suggest that the sand
227 deposition occurred in shallow waters (Savatorini, 1969), yet below the wave base. In
228 the innermost parts of the study area, these deposits lay directly on the Mesozoic
229 limestone; locally, they shade upward into carbonate-cemented sandstones. An up to 2

230 m-thick calcareous sandstone (“Panchina”) overlies either the sandy silt or directly the
231 underlying clayey silt through an erosive contact.

232 Marine Terraced Deposits other than the Sabbie a Brachiopodi are also present in
233 the study area. Along the Ionian side, the two lowermost units are represented by algal
234 biocalcarenites rich in tropical fauna (i.e., *Strombus bubonius* Lamarck, *Cardita*
235 *calyculata senegalensis* Reeve, *Patella ferruginea* Gmelin, *Hyotissa hyotis* Linnaeus,
236 etc.) and reefal build-ups bio-constructed by *Cladocora caespitosa* Linnaeus. This fossil
237 content, and the impressive set of relative (amino acid racemisation) or absolute (U/Th
238 ratio) age determinations associated, indicates a tropical environment of Late
239 Pleistocene age, that corresponds to the MIS 5.5 (Fig. 4). Deposits referred to sub-stages
240 more recent than MIS 5 are also locally exposed (e.g. Hearthy and Dai Pra, 1992;
241 Belluomini et al., 2002, and references therein).

242 Along the Adriatic side of the Murge Plateau and of the Brindisi Plain, well-
243 cemented sterile calcarenites with rare bioturbations are exposed, ascribed to a
244 beach/dune environment. The absence of fossil remains did not allow any
245 biostratigraphic correlation or absolute age determination. A rough chronological
246 constraint is provided by a man-splinted flint found in the *colluvium* underlying the
247 beach-dune deposits and ascribed to the Middle Paleolithic-Mousterian Age. This
248 suggests a Late Pleistocene age, corresponding to a generic MIS 5, for the overlying
249 marine deposits (Marsico et al., 2003).

250 Finally, three generations of dune belts have been referred to the Holocene (Fig.
251 4). In some places they are associated with beach sediments, which can be recognized
252 along several tracts of the Southern Apulia coast (Mastronuzzi and Sansò, 2002b). The
253 oldest dune generation is the most developed; it is represented by aeolian, poorly
254 cemented, bioclastic sands which retain some *Helix* sp. specimens. A number of

255 radiocarbon age determinations on *Helix* sp., integrated with geomorphological and
256 archaeological data, suggest that these dunes formed about 6.5 ka BP, during the
257 maximum flooding event (Flandrian transgression). The second generation of dune
258 belts, made up of loose brownish sands alternating with soil horizons, formed during the
259 Greek-Roman Age. The last phase of dune formation has been ascribed instead to
260 Medieval times.

261

262 Quaternary vertical motions. Within the Quaternary long-term uplift of the Adriatic
263 foreland, which started in the latest Early Pleistocene (Pieri et al., 1996) or during the
264 Middle Pleistocene (Ciaranfi et al., 1983), different landscape units indicate a not
265 homogeneous morphotectonic evolution of the Murge Plateau and Salento Peninsula
266 (Bordoni and Valensise, 1998; Ferranti et al., 2006). This evolution is also accompanied
267 by evidence of pre-, sin- and post-sedimentary tectonic activity, affecting for instance
268 Pleistocene deposits exposed in the surroundings of Bari and Brindisi (Moretti and
269 Tropeano, 1996; Moretti, 2000).

270 The Murge Plateau is bordered by a staircase of well developed marine
271 erosional/depositional terraces, suggesting that the origin of the plateau is related to the
272 effects of eustatic sea level changes superimposed to long-term regional uplift. On the
273 contrary, the Salento Peninsula, although characterized by a set of horst and graben
274 affecting the Mesozoic bedrock (locally named “Serre”; Palmentola, 1987), displays a
275 flat landscape that makes more complex to read the interplay between uplift and
276 eustatism. The Sabbie a Brachiopodi sedimentation has been related to a marked
277 subsidence occurred at least in the western and inner parts of Salento during the Middle
278 Pleistocene (D’Alessandro et al., 1994). A subsequent uplift was then responsible for
279 the emersion of wide sectors of the peninsula. The uplift-rate strongly decreased at MIS

280 9.3, about 330 ka BP (Mastronuzzi et al., 2007b); since then, maximum values of uplift-
281 rate have been recorded only in the Taranto area (0.25 mm/a; Ferranti et al., 2006),
282 whereas they taper to zero in the southernmost part of the region (Dai Pra and Hearthly
283 1988; Hearthly and Dai Pra, 1992; Belluomini et al., 2002). Finally, a slow subsidence
284 seems to characterize at present the Adriatic side of the Apulia region (Mastronuzzi and
285 Sansò, 2002c; Marsico et al., 2003; Lambeck et al., 2004).

286

287 **3. Mesostructural analysis**

288

289 *3.1. Methodological approach*

290

291 This paper deals with brittle fractures characterized by a displacement vector with a
292 prevailing component orthogonal to the fracture surface and a negligible shear
293 component. These tectonic features are here referred to as “extension joints” and are
294 mainly associated with a mode-I propagation mechanism (e.g. Hancock, 1985; Pollard
295 and Aydin, 1988; Engelder, 1994). Only extension joints have been considered in our
296 statistical analyses, that we carried out by applying an inversion technique proposed by
297 Caputo and Caputo (1989) in order to infer the orientation of the principal stress axes
298 and their ratio. The basic assumptions for the application of this numerical method are
299 (i) that two orthogonal joint sets within the same site be genetically related to a unique
300 remote causative stress field, and (ii) that they both consist of pure extension joints.
301 Both assumptions must be verified directly in the field by checking intersection
302 geometries and displacement vectors. In case (i), we observe mutual abutting
303 relationships documenting geologically coeval joint sets, therefore associated with the
304 same remote stress field. In case (ii), we observe that the displacement vectors are

305 systematically at high angle, almost perpendicular to the fracture planes, documenting
306 the opening mode-I and therefore the tensile origin of the joints.

307 The mechanical model is based on the principle that, given a single joint, the
308 principal minimum stress axis σ_3 is perpendicular to the fracture plane while the
309 maximum principal stress axis σ_1 is parallel to it, though with a not determined
310 direction. In case of two coeval orthogonal joints, it is possible to determine the
311 orientation of the σ_1 , which is parallel to the intersection between the planes. When a
312 statistically significant number of joints cluster in two roughly orthogonal sets, an
313 inversion technique can be applied to infer the orientation of the principal stress axes.
314 Coarsely speaking, the “mean” direction of all intersections represents the σ_1 , while the
315 barycenters of the poles to the planes of the two sets represent the remote principal
316 stress axes σ_2 and σ_3 . The σ_3 axis corresponds to the denser cluster of poles (i.e., to the
317 most developed extension joint set). To avoid bias from data collection, we spent an
318 effort to carefully seek 3D outcrops. The use of a least square method and of a Lagrange
319 multiplier assures that the three mean directions are mutually orthogonal as theoretically
320 expected (Caputo and Caputo, 1989).

321 In reality, the fact that two mutually abutting orthogonal joint sets affect a rock
322 mass implies that the stress field has continuously varied during the brittle
323 deformational phase. In particular, as far as the σ_3 is always perpendicular to an
324 extensional joint during its formation, it must have been alternatively oriented in the
325 two directions defined by the two joint sets and inferred by the numerical method. This
326 local variation is explained by a “swap mechanism” caused by the stress release
327 associated with, and intrinsic to, the fracturing process (Caputo, 1995; 2005). As a
328 consequence, although the remote σ_2 and σ_3 are stable in time, when a rock volume
329 undergoes extensional fracturing, the local σ_2 and σ_3 axes temporarily swap,

330 interchanging repeatedly their orientation. Finally, the proposed inversion technique
331 also allows us to calculate the ratio $R = (\sigma_2 - \sigma_3)/(\sigma_1 - \sigma_3)$, which is an important
332 parameter indicative of the shape of the mean stress ellipsoid.

333 The proposed methodological approach shows a limitation when applied to sites
334 where only one joint set occurs with an associated $R \cong 1$. In these cases, we cannot rule
335 out the hypothesis that $\sigma_1 \neq \sigma_2$, because it is also possible that σ_1 and σ_2 absolute values
336 did not allow the inception of the stress swap mechanism. Accordingly, the stress tensor
337 could be triaxial and, in principle, correspond to either a normal Andersonian regime (σ_z
338 $= \sigma_1$) or a transcurent one ($\sigma_z = \sigma_2$).

339

340 *3.2. Paleostresses from extensional joints analysis*

341

342 In order to get information about the Middle-Late Quaternary tectonic evolution of the
343 study region, we investigated numerous sites by measuring the joint orientations and
344 their opening vectors. Observations have been made both on sub-horizontal surfaces
345 and on two or more vertical sections views, thus attempting a 3D vision of the outcrops,
346 which were often represented by quarries (Figs. 4 and 5). In particular, the analysis of
347 the quarry floors allowed a correct interpretation of the number and organization of the
348 orthogonal joint sets measured along the walls, avoiding to undersample one of the two
349 sets. To guarantee statistically reliable results of the quantitative analyses, for each site
350 we measured as many joints as possible, ensuring a minimum of 20-30 fractures per
351 joint system. Particular care was spent in the field to check the possible occurrence
352 (indeed never detected) of horizontal extensional joints. Figure 6 shows some examples
353 of the analyzed joint systems, where fractures are plotted as poles to the planes in
354 stereographic projections (lower hemisphere). The principal stress axes, σ_1 , σ_2 and σ_3 ,

355 are represented as triangles, rhombi and squares, respectively. The size of the symbols
356 is proportional to the amount of opening and length of the joints, as measured in the
357 field. This information has been included in the numerical inversions as a statistical
358 weight because, when dealing with extensional veins, both cumulative opening and total
359 length are somehow proportional to the number of fracturing events occurred and hence
360 to the remote tensile conditions.

361 Similar to most inversion techniques used in mesostructural analyses (Carey and
362 Brunier, 1974; Angelier, 1975; Etchecopar et al., 1981; Armijo et al., 1982; Reches,
363 1987; Caputo and Caputo, 1988; Huang, 1989), also the method applied in this paper
364 (Caputo and Caputo, 1989) follows the assumption that the amount of displacement (in
365 our case, of opening) associated with the fracture system is negligible with respect to
366 the dimensions of the investigated rock volume. If such assumption must be carefully
367 verified in the field when analyzing faults, it is obvious for the sites considered in this
368 work, which are affected only by extension joints. As an often implicit consequence of
369 this general assumption, the calculated strain tensor can be considered co-axial with the
370 causative stress tensor and hence a kinematic information like the amount of opening
371 can be safely used as a statistical weight. A further reason for using opening and joint
372 length in the numerical inversion follows the observation that large and thick veins are
373 commonly the result of several rupture events (Caputo and Hancock, 1999). We do not
374 consider joint spacing (or density) because it mainly depends on the distribution of
375 subsequent fracturing events (e.g. crack-seal versus crack-jump mechanisms) and not on
376 the remote tensile stress.

377 In the numerous sites investigated, the extension joints form sets of nearly parallel
378 planes. Locally a unique joint set was recognized (Fig. 6a), but the occurrence of two
379 well developed, roughly orthogonal sets is more common (Fig. 6b). In few but crucial

380 cases, more than two joint sets exist (Fig. 6c and d).

381 Following the basic concepts proposed by Hancock (1985) to determine the relative
382 timing of fractures, in the field we spent particular care to observe the occurrence of
383 mutual or systematic abutting relationships between joints belonging to different sets
384 (Fig. 5). Accordingly, we considered the corresponding joint sets as geologically coeval
385 or not, respectively. In the former case, the two joint sets have been analyzed as a
386 unique joint system, while in the latter case the two sets have been separated before
387 performing the numerical inversions (Fig. 6c and d).

388

389 **4. Discussion**

390

391 Based on the mesostructural analysis of the Quaternary deposits cropping out in Salento
392 and on the numerical inversions of the acquired datasets, our results suggest some
393 immediate simple considerations. Firstly, all the “local” stress tensors calculated for
394 each site are characterized by a vertical maximum principal stress axis (σ_1), therefore
395 documenting the occurrence of an extensional tectonic regime (*sensu* Anderson, 1942)
396 throughout the entire area. Secondly, the two horizontal principal stress axes (σ_2 and
397 σ_3), although variably oriented in the different sites, show some recurrent directions.
398 Thirdly, in some sites we observed two distinct joint systems, that we interpret as the
399 result of different stress fields occurred in subsequent periods. These considerations are
400 developed in the following.

401

402 *4.1. Tectonic stratigraphy*

403

404 The “tectonic stratigraphy” of an area is defined as the structural evolution that can be

405 reconstructed for that zone by determining (i) the number of deformational events
406 occurred in a given time interval, (ii) the related stress trajectories or the average stress
407 field, (iii) the areal distribution of the associated deformation structures, i.e., the
408 dimensions of the crustal volume involved, and (iv) in case of two or more events, their
409 relative and absolute chronology (Caputo and Pavlides, 1993).

410 In this perspective, we can reconstruct the Middle and Late Quaternary tectonic
411 stratigraphy of the southern Adriatic foreland of Italy, as all the studied sites have been
412 selected exclusively in carbonate deposits not older than the late Lower Pleistocene.
413 This choice allows a detailed chronology of the most recent deformational events,
414 although it implies a scattered distribution of the sites suitable for the structural
415 analysis.

416 By integrating such analysis of the extension joints with geological and litho-
417 stratigraphic information, we were able to organize our dataset in three subsets of data.
418 For each subset, the corresponding mesostructural analysis returned fairly uniform
419 results, indicating the occurrence of at least three separate deformational events during
420 the Middle and Late Quaternary. These three subsets are shown separately in Tables 1
421 to 3 (from the oldest to the most recent deformational event, respectively) and in the
422 corresponding Figure 7a, b and c. We will discuss each subset individually.

423 In the tables, the occurrence within the same site of two distinct joint systems is also
424 emphasized in the column “*relative age*”. In this case, the relative chronology is also
425 indicated, as evaluated in the field. Moreover, on the right-hand columns, for each site
426 we reported the directions of the three principal stress axes and the stress ratio R.

427 The first subset of data includes six sites with horizontal σ_2 and σ_3 roughly trending
428 N-S and/or E-W (Tab. 1). These localities are distributed all over the investigated area
429 (Fig. 7a), therefore suggesting the regional significance of this deformational event. In

430 many cases, the E-W joint set dominates, while locally the N-S prevails (e.g. Sal034,
431 where, however, local effects cannot be ruled out). In all cases, extension is almost
432 uniaxial, as documented by the ratio R that varies in the 0.64-0.99 interval, with
433 prevailing values near the upper bound. Abutting relationships with the other joints
434 analyzed show that the joint sets belonging to this first subset of data are constantly
435 older than the other ones. Moreover, they were never observed in rocks younger than
436 the late Lower Pleistocene. Taking into account the age of the hosting deposits and the
437 age of the second subset of data (see below in this same section), the deformational
438 event represented by the first subset of data is constrained to the early and middle part
439 of the Middle Pleistocene.

440 The stress variability observed within this subset could be tentatively explained in
441 different ways. Firstly, it could be artificial, i.e., we grouped not coeval stress fields.
442 However, the relatively tight chronological constraint does not favour this hypothesis,
443 that would assume the occurrence of more than one deformational event in a very short
444 time window. Secondly, as far as all the measured stress fields are representative of
445 very superficial crustal rocks, they were characterized by low magnitude stresses.
446 Therefore, they could have been very sensitive to local effects due, for example, to
447 underlying inherited structures, lithological variations or morphological irregularities.
448 However, the relatively limited number of investigated sites does not help to definitely
449 confirm this explanation. Thirdly, as above discussed, when $R \cong 1$ and only one joint set
450 occurs (as in the cases of sites Sal061 and Sal067; Fig. 7a), the possibility that the stress
451 tensor be triaxial and the tectonic regime purely tensional ($\sigma_z = \sigma_1$) or transcurrent ($\sigma_z =$
452 σ_2) cannot be ruled out.

453 The second subset of data has been observed in ten sites (Fig. 7b and Tab. 2). The
454 estimated stress tensors are characterized by an almost uniaxial tension, represented by

455 an ellipsoid of revolution around the horizontal σ_3 axis. The orientation of the least
456 principal stress ranges between N22° and N62°, with a mean value of ~N43° (Fig. 8).
457 The stress ratio R is high, ranging between 0.85 and 0.99. Also in this case, due to
458 method limitations, the occurrence of sites with only one joint set (e.g. Sal066 and
459 Sal069; Fig. 7b) explains the local misorientation of the σ_1 and σ_2 axes, that could be
460 part of a triaxial tensor. This NE-SW extension characterizes the Early-Middle
461 Pleistocene rocks whereas it was never observed in Late Quaternary deposits. Based on
462 sites characterized by more than one joint system (e.g. site Sal072), this event is clearly
463 older than the deformational event associated with the third subset of data, while it is
464 younger than the joint system belonging to the first subset of data (Sal012 and Sal064).
465 Therefore, a late Middle Pleistocene age can be reasonably assigned to this
466 deformational event.

467 The third subset of data includes twelve sites covering the entire investigated area
468 (Fig. 7c and Tab. 3). The common feature which characterizes the sites of this subset is
469 a low R ratio, with values that never exceed 0.47 and are frequently lower than 0.30.
470 Such values correspond to an ellipsoid that tends to be of revolution around the σ_1
471 vertical axis; the σ_2 and σ_3 axes are comparable, thus indicating a sort of horizontal
472 ‘radial’ extension. Even though the remote σ_2 and σ_3 axes were quite similar in
473 magnitude, at least as a space and time average, due to the stress swap mechanism the
474 related joints commonly cluster in two roughly orthogonal sets statistically equivalent.

475 All the youngest investigated sites, consisting of Upper Pleistocene calcarenites, are
476 included in this subset, whereas sites characterized by older Quaternary deposits show
477 systematic abutting relationships. Accordingly, this deformational event is not older
478 than the Late Pleistocene and possibly reflects the active stress field still pervading (at
479 least) the shallower sectors of the entire study area.

480 We consider unlikely the hypothesis of this event as resulting from the
481 superposition of local conditions on a regional stress field analogous to that associated
482 to the second event. Beyond the difference in age of the affected deposits, many of the
483 sites coincide in the two subsets, and this rules out possible local causes at the outcrop
484 scale. Moreover, the wide distribution of the third subset of data all over the study area
485 can be better explained by a large scale cause.

486

487 *4.2. Geodynamic perspective*

488

489 From a seismotectonic point of view, the documented mild deformation, joined with the
490 lack of major, active, emergent faults (e.g. like the Mattinata fault in the Gargano
491 Promontory; Fig. 1) and with the scarce historical and instrumental seismicity (Fig. 2),
492 do not favour the hypothesis of large seismogenic sources in the study area, whereas the
493 occurrence of moderate earthquakes cannot be ruled out. Moreover, with regard to the
494 recent geodynamics of the southern Adriatic foreland, we observe that, within a general
495 extension, during the Middle and Late Pleistocene our study area underwent second
496 order yet detectable variations of the principal stress axes with time intervals in the
497 order of few hundred ka. Comparable variations affecting the southern Adriatic foreland
498 during the Middle and Late Quaternary have been already suggested for a sector north
499 of our study area, the Gondola fault zone in the Gargano off-shore (Fig. 1). In this zone,
500 Ridente and Trincardi (2006) and Ridente et al. (2008) infer analogous intensity
501 variations of the tectonic activity along the fault zone, and recognize a relative
502 maximum of deformation in the latest Middle Pleistocene (230-250 to 130-140 ka),
503 followed by a still evident yet less intense tectonic activity. This independent result
504 confirms what suggested by our data, i.e., the recent tectonic evolution of the southern

505 Adriatic foreland is marked by weak deformation whose intensity varies through time
506 sufficiently to determine surface evidence of this variation.

507 The oldest deformational event found (Fig. 8a) is referred to the early and middle
508 part of the Middle Pleistocene. As mentioned in the previous sections, in the same time
509 interval the Southern Apennines were just undergoing a geodynamic change
510 characterized by (i) the inception of a SW-NE extension over the chain ridge, (ii) the
511 end of the east-northeastward motion of the wedge front in the Bradanic foredeep, and
512 (iii) the beginning of a long-term uplift in the Apulia region. The oldest deformational
513 event could be thus interpreted as the response of the foreland to the contractional
514 regime responsible for the last motion of the Southern Apennines front (Patacca and
515 Scandone, 2004; Fig. 1).

516 The penultimate deformational event is referred to the latest Middle Pleistocene and
517 is characterized by a SW-NE extension accompanied by high R values (Fig. 8b). This
518 extension is widespread and characterised by well organized and defined pattern of
519 planes, with limited dispersion with respect to the dominant direction. From a regional
520 perspective, a SW-NE extension is not surprising. For instance, NW-SE graben
521 structures involving Plio-Quaternary deposits off-shore, southeast of Salento, have
522 already been described by Argnani et al. (2001). The same investigators interpret this
523 deformation as an outer-arc extension due to the flexure of the Adriatic foreland.

524 Different causes have been proposed in the literature for this flexure, showing
525 that the debate on the geodynamics of the Adriatic block is indeed a lively one, but also
526 that for this tectonic domain the Middle and Late Quaternary geodynamic evolution has
527 always been considered as a whole, without more detailed analyses. For instance:

- 528 1. Billi and Salvini (2003) consider the flexure of Apulia as the on-shore forebulge of
529 the Adriatic foreland, and interpret in this perspective of flexural processes the NW-
530 SE systematic joints measured in the Mesozoic carbonate rocks.
- 531 2. Various investigators invoke the buckling of a thick continental lithosphere as a
532 possible cause, either within an active subduction beneath the Southern Apennines
533 (Doglioni et al., 1994) or due to horizontal compression, also associated with the
534 Albanides convergence (Bertotti et al., 2001).
- 535 3. Moreover, although most researchers set the end of Southern Apennines thrusting
536 around the beginning of the Middle Pleistocene (e.g. Butler et al., 2004; Patacca and
537 Scandone, 2004), others contend that at that time thrusting did not cease and possibly
538 shifted to the northeast, progressively involving the Adriatic “foreland” (Caputo and
539 Bianca, 2005; Ferranti and Oldow, 2006; Caputo et al., 2007). Within this latter
540 scenario, SW-NE extension could be explained as the result of a crustal-scale
541 extrados stretching, that is to say, as the surface evidence of a deep ramp anticline
542 associated with a thrust detachment rooting within the crystalline part of the Adriatic
543 crust.
- 544 4. Besides, the Salento and its off-shore counterpart form the flexural bulge of the
545 eastern, lateral portion of the Calabrian arc (Doglioni et al., 1999), that is an orogenic
546 wedge associated with a subducting slab of oceanic lithosphere (Faccenna et al.,
547 2003, with references). The recent SW-NE extension of our study area could also be
548 related to this deeper engine.
- 549 5. Finally, since the Late Tortonian the general geodynamic frame of the Adriatic
550 foreland is dominated by the Africa motion toward stable Europe along NNW-SSE
551 to NW-SE vectors (e.g. Mazzoli and Helman, 1994). The SW-NE extension of the
552 study area could also be interpreted as a consequence of this convergence.

553 Summarizing, all these geodynamic models justify a SW-NE active extension in
554 the study area. On the one hand, our data confirm this extension and supply new
555 chronological constraints for its activity; on the other hand, they obviously cannot
556 provide the key to define a preferred geodynamic model.

557 All these models can be also compared with the most recent deformational event
558 described in this work (Fig. 8c), characterized by low R ratio and by a horizontal,
559 almost radial extension (*viz.* comparable σ_2 and σ_3), emphasized by the high angular
560 deviation of σ_2 and σ_3 ($\pm 54^\circ$ in both cases, with 18° overlap, therefore totally
561 interchangeable from a statistical point of view). If we compare this sort of “doming” of
562 the study area with the previous deformational event, we have to hypothesize a Late
563 Pleistocene stress field variation which encompasses a relative decrease of the σ_2 with
564 respect to the σ_3 (or increase of the σ_3 with respect to the σ_2). This kind of evolution and
565 the final doming observed suggest a geodynamic setting where two orthogonal engines
566 compete (Fig. 9).

567 The ongoing slab subduction beneath the Calabrian arc is outlined by seismicity
568 data (Giardini and Velonà, 1991; Castello et al., 2005), and the related wedge front
569 deforms the seafloor in the Ionian Sea (Doglioni et al., 1999). In the Taranto Gulf, the
570 Calabrian wedge is in structural continuity with the Southern Apennines wedge (Bigi et
571 al., 1990; Figs. 2 and 9). Tilted Upper Pleistocene marine deposits suggest a possible
572 weak activity also for the latter wedge (Caputo et al., 2007). This activity should taper
573 to zero moving towards the NW, where according to Patacca and Scandone (2004) the
574 migration of the Southern Apennines toward the Adriatic foreland ceased at the
575 beginning of the Middle Pleistocene (~650 ka). Along the northeastern side of the
576 Adriatic Sea, the compressional regime presently affecting the Dinarides, Albanides and
577 the northern Hellenides fold-and-thrust belts is well depicted by the relevant seismicity

578 and related focal mechanisms (Harvard CMT Project 2006). Finally, the current
579 geodynamic frame of the Adriatic foreland is still dominated by the NW-SE Eurasia-
580 Nubia convergence (Serpelloni et al., 2007; Devoti et al., 2008; Fig. 9). This
581 convergence has been interpreted as responsible for the active deformation of other
582 parts of the Adriatic foreland (e.g. the MSsz; Di Bucci and Mazzoli, 2003; Valensise et
583 al., 2004; Di Bucci et al., 2006; Ridente et al., 2008) and it is compatible with the
584 seismicity recorded on-land in different parts of the southern Adriatic foreland, both
585 exposed and inflected below the outer front of the southern Apennines (Borre et al.,
586 2003; Di Luccio et al., 2005; Del Gaudio et al., 2005; 2007; Boncio et al., 2007).

587 On these bases, the two engines hypothesized could be tentatively found on the
588 one hand in the Calabrian arc (in particular its lateral portion in the Taranto Gulf) and
589 Dinarides-Albanides-Hellenides chain, and on the other hand in the NW-SE Eurasia-
590 Nubia convergence (Fig. 9). Together, they could provide the competing horizontal
591 forces needed to determine the observed doming and the consequent fibre stresses (e.g.
592 Argnani et al., 2001; Billi and Salvini, 2003).

593

594 **5. Final remarks**

595

596 The method applied in this work to study orthogonal extensional joints turns out to be
597 suitable for the analysis of the recent-to-active stress field in foreland areas affected by
598 mild deformation. The southern Adriatic foreland of Italy has a crucial location in the
599 Central Mediterranean tectonic domains. Therefore, the identification of the recent (-to-
600 active) stress field of this region, mild but not negligible as considered up to now, can
601 provide a key to interpret the relationships among these tectonic domains. For the
602 Middle and -at least- Late Pleistocene, our results suggest an overall homogeneous

603 framework of shallow (upper crustal) extension, with three deformational events of
604 regional significance that can be recognized within this general extensional regime.

605 The oldest event, constrained to the early and middle part of the Middle
606 Pleistocene, is characterized by variable direction of extension. The penultimate event,
607 dated late Middle Pleistocene, is characterized by an almost uniaxial tension, with a
608 horizontal σ_3 striking SW-NE. The most recent event is characterized by a horizontal
609 ‘radial’ extension; it is not older than the Late Pleistocene and possibly reflects the
610 active stress field still dominating the entire study area. The deformation associated with
611 this stress field can be described as a sort of doming, and it has been tentatively
612 explained as the result of two geodynamic far-ranging components that act
613 simultaneously: (i) the Calabrian arc and the Dinarides-Albanides-Hellenides chain, and
614 (ii) the NW-SE Eurasia-Nubia convergence. Together, they could provide the
615 competing horizontal stresses needed to determine the observed doming of this crustal
616 i.e. rigid block.

617

618 **Acknowledgments**

619 Thanks are due to P. Boncio, D. Peacock, G. Roberts and G. Valensise for criticisms and fruitful
620 discussions. The work benefited from the constructive review by J. Galindo-Zaldivar, A.M.
621 Michetti and the Editor L. Piccardi, who are kindly acknowledged. Study supported by the
622 Project S2 funded in the framework of the 2004-2006 agreement between the Italian
623 Department of Civil Protection and the INGV (Research Units 2.4-Burrato, 2.11-Mastronuzzi).
624 Scientific papers funded by DPC do not represent its official opinion and policies.

625

626 **References**

- 627 Anderson, E.M., 1942. The dynamics of faulting and dyke formation with applications
628 to Britain. Oliver and Boyd, 191 pp., Edinburgh.
- 629 Angelier, J., 1975. Sur un apport de l'informatique à l'analyse structurale: exemple de la
630 tectonique cassante. *Revue de Géographie Physique et de Géologie Dynamique*
631 17 (2), 137-146.
- 632 Argnani, A., Rugosi, F., Cosi, R., Ligi, M., Favali, P., 2001. Tectonics and seismicity of
633 the Apulian Ridge south of Salento peninsula (Southern Italy). *Annals of*
634 *Geophysics* 44, 527-540.
- 635 Armijo, R., Carey, E., Cisternas, A., 1982. The inverse problem in microtectonics and
636 the separation of tectonic phases. *Tectonophysics* 82, 145-160.
- 637 Belluomini, G., Caldara, M., Casini, C., Cerasoli, M., Manfra, L., Mastronuzzi, G.,
638 Palmentola, G., Sansò, P., Tuccimei, P., Vesica, P.L., 2002. The age of Late
639 Pleistocene shorelines and tectonic activity of Taranto area, Southern Italy.
640 *Quaternary Science Reviews* 21, 525-547.
- 641 Bertotti, G., Picotti, V., Chilovi, C., Fantoni, R., Merlini, S., Mosconi, A., 2001.
642 Neogene to Quaternary sedimentary basins in the south Adriatic (Central
643 Mediterranean): foredeeps and lithospheric buckling. *Tectonics* 20 (5), 771-787.
- 644 Bigi, G., Cosentino, D., Parotto, M., Sartori, R., Scandone, P., 1990. Structural Model
645 of Italy and Gravity Map. CNR, P.F. Geodinamica, Quaderni de "La ricerca
646 scientifica" 114, 3, six sheets.
- 647 Billi, A., Salvini, F., 2003. Development of systematic joints in response to flexure
648 related fibre stress in flexed foreland plates: the Apulian forebulge case history,
649 Italy. *Journal of Geodynamics* 36, 523-536.
- 650 Boncio, P., Mancini, T., Lavecchia, G., Selvaggi, G., 2007, Seismotectonics of strike-
651 slip earthquakes within the deep crust of southern Italy: geometry, kinematics,
652 stress field and crustal reology of the Potenza 1990-1991 seismic sequences.
653 *Tectonophysics*, doi: 10.1016/j.tecto.2007.08.016.
- 654 Bordoni, P., Valensise, G., 1998. Deformation of the 125 ks marine terrace in Italy:
655 tectonic implications. In: Stewart, I.S., Vita Finzi, C. (Eds.), *Coastal Tectonics*.
656 Geological Society, London, Special Publications 146, 71-110.
- 657 Borre, K., Cacon, S., Cello, G., Kontny, B., Kostak, B., Likke Andersen, H., Moratti,
658 G., Piccardi, L., Stemberk, J., Tondi, E., Vilimek, V., 2003, The COST project in
659 Italy: analysis and monitoring of seismogenic faults in the Gargano and Norcia
660 areas (central-southern Apennines, Italy). *Journal of Geodynamics* 36, 3-18.
- 661 Bossio, A., Mazzei, R., Monteforti, B., Salvatorini, G., 1991. Note geologiche e
662 stratigrafiche sull'area di Palmariggi (Lecce, Puglia). *Rivista Italiana di*
663 *Paleontologia Stratigrafica* 97 (2), 175-234.
- 664 Butler, R.W.H., Mazzoli, S., Corrado, S., De Donatis, M., Scrocca, D., Di Bucci, D.,
665 Gambini, R., Naso, G., Nicolai, C., Shiner, P., Zucconi, V., 2004. Applying thick-
666 skinned tectonic models to the Apennine thrust belt of Italy - Limitations and
667 implications: In: McClay, K. (Ed.), *Thrust tectonics and hydrocarbon systems*.
668 American Association of Petroleum Geologists Memoir 82, 647-667.

- 669 Capaldi, G., Civetta, L., Lirer, L., Munno, R., 1979. Caratteri Petrografici ed età K/Ar
670 delle cineriti intercalate nelle formazioni argillose pleistoceniche della Fossa
671 Bradanica. *Geologia Applicata ed Idrogeologia* 14 (3), 493-501.
- 672 Caputo, M., Caputo, R., 1988. Structural analysis: new analytical approach and
673 applications. *Annales Tectonicae* 2 (2), 84-89.
- 674 Caputo, M., Caputo, R., 1989. Estimate of the regional stress field using joint systems.
675 *Bulletin of the Geological Society of Greece* 23 (1), 101-118.
- 676 Caputo, R., 1995. Evolution of orthogonal sets of coeval extension joints. *Terra Nova* 7
677 (4), 479-490.
- 678 Caputo, R., 2005. Stress variability and brittle tectonic structures. *Earth-Science
679 Reviews* 70 (1-2), 103-127.
- 680 Caputo, R., Bianca, M., 2005. Morphological evidence of Late Quaternary thrusting in
681 the Bradanic Foredeep. *Rend. Soc. Geol. It.*, 1, nuova serie, 75-76.
- 682 Caputo, R., Hancock, P.L., 1999. Crack-jump mechanism of microvein formation and
683 its implications for stress cyclicity during extension fracturing. *Journal of
684 Geodynamics* 27, 45-60.
- 685 Caputo, R., Pavlides, S., 1993. Late Cainozoic geodynamic evolution of Thessaly and
686 surroundings (Central-Northern Greece). *Tectonophysics* 223 (3-4), 339-362.
- 687 Caputo, R., Bianca, M., D'Onofrio, R., 2007. Is the orogenic activity still active in the
688 external Southern Apennines?. 6th Forum GeoItalia, Rimini, September 11-15,
689 2007. *Epitome* 2, 236.
- 690 Carey, E., Brunier, B., 1974. Analyse théorique et numérique d'un modèle mécanique
691 élémentaire appliqué à l'étude d'une population de failles. *Comptes rendus de
692 l'Académie des Sciences de Paris* D279, 891-894.
- 693 Castello, B., Selvaggi, G., Chiarabba, C., Amato, A., 2005. CSI, Catalogo della
694 sismicità italiana 1981-2002, versione 1.0. INGV-CNT, Roma.
695 <http://www.ingv.it/CSI/>
- 696 Ciaranfi, N., Ghisetti, F., Guida, M., Iaccarino, G., Lambiase S., Pieri, P., Rapisardi, L.,
697 Ricchetti, G., Torre, M., Tortorici, L., Vezzani, L., 1983. Carta Neotettonica
698 dell'Italia Meridionale. *CNR, P.F. Geodinamica* 515, 1-62.
- 699 Ciaranfi, N., Pieri, P., Ricchetti, G., 1988. Note alla carta geologica delle Murge e del
700 Salento (Puglia centro-meridionale), 1:250.000. *Memorie della Società Geologica
701 Italiana* 42, 449-460.
- 702 Ciaranfi, N., Pasini, G., Rio, D., 2001. The meeting on the Plio-Pleistocene boundary
703 and the Lower/Middle Pleistocene transition: type areas and sections (Bari, 25-29
704 September 2000). *Memorie di Scienze Geologiche* 53, 1-123.
- 705 Cinque, A., Patacca, E., Scandone, P., Tozzi, M., 1993. Quaternary kinematic evolution
706 of the southern Apennines. Relationship between surface geological features and
707 deep lithospheric structures. *Annali di Geofisica* 36, 249-260.
- 708 Console, R., Di Giovambattista, R., Favali, P., Presgrave, B.W., Smriglio, G., 1993.
709 Seismicity of the Adriatic microplate. *Tectonophysics* 218, 343-354.

- 710 Coppa, M.G., De Castro, P., Marino, M., Rosso, A., Sanfilippo, R., 2001. The
711 Pleistocene with *Aequipecten opercularis* (Linneo) of “Campo di Mare” (Brindisi,
712 Italy). *Bollettino della Società Paleontologica Italiana* 40 (3), 405-429.
- 713 D'Alessandro, A., Iannone, A., 1982. Pleistocene carbonate deposits in the area of
714 Monopoli (Bari Province): sedimentology and palaeocology. *Geologica Romana*
715 21, 603-653.
- 716 D'Alessandro, A., Iannone, A., 1984. Prime considerazioni sedimentologiche e
717 paleoecologiche su alcune sezioni della Calcarenite di Gravina (Pleistocene) nei
718 pressi di Monopoli. *Studi di Geologia e Geofisica* 27, 1-16.
- 719 D'Alessandro, A., Massari, F., 1997. Pliocene and Pleistocene depositional
720 environments in the Pesculuse area (Salento, Italy). *Rivista Italiana di*
721 *Paleontologia e Stratigrafia* 103, 221-258.
- 722 D'Alessandro, A., Palmentola, G., 1978. Sabbie e Brachiopodi, una nuova unità del
723 Salento leccese (aspetti litosfratigrafici e paleoambientali). *Rivista Italiana di*
724 *Paleontologia e Stratigrafia* 84, 1083-1120.
- 725 D'Alessandro, A., Mastronuzzi, G., Palmentola, G., Sansò, P., 1994. Pleistocene
726 deposits of Salento leccese (Southern Italy): problematic relationships. *Bollettino*
727 *della Società Paleontologica Italiana* 33 (2), 257-263.
- 728 Dai Pra, G., and Hearty, P.J., 1988. I livelli marini pleistocenici del Golfo di Taranto,
729 sintesi geocronostratigrafica e tettonica. *Memorie della Società Geologica Italiana*
730 41, 637-644.
- 731 Del Gaudio, V., Pierri, P., Calcagnile, G., Venisti, N., 2005. Characteristics of the low
732 energy seismicity of central Apulia (southern Italy) and hazard implications.
733 *Journal of Seismology* 9, 39-59.
- 734 Del Gaudio, V., Pierri, P., Frepoli, A., Calcagnile, G., Venisti, N., Cimini, G.B., 2007.
735 A critical revision of the seismicity of Northern Apulia (Adriatic microplate -
736 Southern Italy) and implications for the identification of seismogenic structures.
737 *Tectonophysics* 436, 9-35.
- 738 Devoti, D., Riguzzi, F., Cuffaro, M., Doglioni, C., 2008. New GPS constraints on the
739 kinematics of the Apennines subduction. *Earth Planet. Sci. Lett.* 273, 163-174.
- 740 Di Bucci, D., Mazzoli, S., 2003. The October-November 2002 Molise seismic sequence
741 (southern Italy): an expression of Adria intraplate deformation. *Journal of the*
742 *Geological Society London* 160, 503-506.
- 743 Di Bucci, D., Ravaglia, A., Seno, S., Toscani, G., Fracassi, U., Valensise, G., 2006.
744 Seismotectonics of the Southern Apennines and Adriatic foreland: insights on
745 active regional E-W shear zones from analogue modelling. *Tectonics* 25, TC4015,
746 doi: 10.1029/2005TC001898.
- 747 Di Bucci, D., Coccia, S., Fracassi, U., Iurilli, V., Mastronuzzi, G., Palmentola, G.,
748 Sansò, P., Selleri, G., Valensise, G., 2009a. Late Quaternary deformation of the
749 southern Adriatic foreland (southern Apulia) from mesostructural data:
750 preliminary results. *Bollettino della Società Geologica Italiana (Italian Journal of*
751 *Geosciences)* 128 (1), 33-46.
- 752 Di Bucci, D., Ridente, D., Fracassi, U., Trincardi, F., Valensise, G., 2009b. Marine
753 paleoseismology from Very High Resolution seismic imaging: the Gondola Fault

- 754 Zone (Adriatic foreland). *Terra Nova* 21 (5), 393-400. doi: 10.1111/j.1365-
755 3121.2009.00895.x
- 756 Di Luccio, F., Fukuyama, E., Pino, N.A., 2005. The 2002 Molise earthquake sequence:
757 what can we learn about the tectonics of southern Italy?. *Tectonophysics* 405,
758 141-154.
- 759 DISS Working Group, 2007. Database of Individual Seismogenic Sources (DISS),
760 Version 3.0.4: A compilation of potential sources for earthquakes larger than M
761 5.5 in Italy and surrounding areas. <http://www.ingv.it/DISS/>, © INGV 2005, 2007.
762 All rights reserved.
- 763 Doglioni, C., Mongelli, F., Pieri, P., 1994. The Puglia uplift (SE-Italy): an anomaly in
764 the foreland of the Apenninic subduction due to buckling of a thick continental
765 lithosphere. *Tectonics* 13, 1309-1321.
- 766 Doglioni, C., Merlini, S., Cantarella, G., 1999. Foredeep geometries at the front of the
767 Apennines in the Ionian Sea (central Mediterranean). *Earth and Planetary Science*
768 *Letters* 168, 243-254.
- 769 Engelder, T., 1994. Brittle crack propagation. In: Hancock, P.L. (Ed.), *Continental*
770 *Deformation*. Pergamon Press, Oxford, 43-52.
- 771 Etchecopar, A., Vasseur, G., Daignieres, M., 1981. An inverse problem in
772 microtectonics for the determination of stress tensors from fault striation analysis.
773 *Journal of Structural Geology* 3 (1), 51-65.
- 774 Faccenna, C., Jolivet, L., Piromallo, C., Morelli, A., 2003. Subduction and the depth of
775 convection in the Mediterranean mantle. *Journal of Geophysical Research* 108
776 (B2), 2099, doi:10.1029/2001JB001690.
- 777 Ferranti, L., Oldow, J.S., 2006. Rates of late Neogene deformation along the
778 southwestern margin of Adria, southern Apennines orogen, Italy, *in* Pinter, N., et
779 al., eds., *The Adria Microplate: GPS Geodesy, Tectonics, and Hazards*. Springer,
780 NATO Science Series IV, 61, 109-131.
- 781 Ferranti, L., Antonioli, F., Mauz, B., Amorosi, A., Dai Pra, G., Mastronuzzi, G.,
782 Monaco, C., Orrù, P., Pappalardo, M., Radtke, U., Renda, P., Romano, P., Sansò,
783 P., Verrubbi, V., 2006. Markers of the last interglacial sea-level high stand along
784 the coast of Italy: Tectonic implications. *Quaternary International* 145-146, 30-54.
- 785 Fracassi, U., Valensise, G., 2007. Unveiling the sources of the catastrophic 1456
786 multiple earthquake: Hints to an unexplored tectonic mechanism in Southern
787 Italy. *Bulletin of the Seismological Society of America* 97 (3), 725-748.
- 788 Funicello, R., Montone, P., Parotto, M., Salvini, F., Tozzi, M., 1991. Geodynamical
789 evolution of an intra-orogenic foreland: the Apulia case history (Italy). *Bollettino*
790 *della Società Geologica Italiana* 110, 419-425.
- 791 Giardini, D., Velonà, M., 1991. Deep seismicity of the Tyrrhenian Sea. *Terra Nova* 3,
792 57-64.
- 793 Gruppo di Lavoro CPTI, 2004. *Catálogo Parametrico dei Terremoti Italiani, vers. 2004*
794 *(CPTI04)*. INGV, Bologna, <http://emidius.mi.ingv.it/CPTI/>
- 795 Guidoboni, E., Ferrari, G. 2004. *Revisione e integrazione di ricerca riguardante il*
796 *massimo terremoto storico della Puglia: 20 febbraio 1743. RPT 272A/05, SGA –*
797 *Storia Geofisica Ambiente, Bologna, 103 pp.*

- 798 Hancock, P.L., 1985. Brittle microtectonics: principles and practice. *Journal of*
799 *Structural Geology* 7 (3-4), 437-457.
- 800 Harvard University, 2006. Harvard Centroid-Moment Tensor Project.
801 <http://www.seismology.harvard.edu/projects/CMT/>
- 802 Hearty, P.J., Dai Pra, G., 1992. The age and stratigraphy of Quaternary coastal deposits
803 along the gulf of Taranto (south Italy). *Journal of Coastal Research* 8 (4), 882-
804 905.
- 805 Hippolyte, J.-C., Angelier, J., Roure, F., 1994. A major geodynamic change revealed by
806 Quaternary stress patterns in the Southern Apennines (Italy). *Tectonophysics* 230,
807 199-210.
- 808 Huang, Q., 1989. Modal and vectorial analysis for determination of stress axes
809 associated with fault slip data. *Mathematical Geology* 21 (5), 543-558.
- 810 Iannone, A., Pieri, P., 1979. Considerazioni critiche sui "Tufi calcarei" delle Murge.
811 Nuovi datii litostratigrafici e paleoambientali. *Geografia Fisica e Dinamica*
812 *Quaternaria* 2, 173-186.
- 813 Lambeck, K., Anzidei, M., Antonioli, F., Benini, A., Esposito, E., 2004. Sea level in
814 Roman time in the Central Mediterranean and implications for modern sea level
815 rise. *Earth and Planetary Science Letters* 224, 563-575.
- 816 Maiorano, P., Aiello, G., Barra, D., Di Leo, P., Joannin, S., Lirer, F., Marino, M.,
817 Pappalardo, A., Capotondi, L., Ciaranfi, N., Stefanelli, S., 2008.
818 Paleoenvironmental changes during sapropel 19 (i-cycle 90) deposition:
819 Evidences from geochemical, mineralogical and micropaleontological proxies in
820 the mid-Pleistocene Montalbano Jonico land section (southern Italy).
821 *Palaeogeography, Palaeoclimatology, Palaeoecology* 257(3), 308-334. doi:
822 10.1016/j.palaeo.2007.10.025S0031-0182(07)00543-3.
- 823 Marino, M., 1996. Quantitative calcareous nannofossil biostratigraphy of the Lower-
824 Middle Pleistocene, Montalbano Jonico section (Southern Italy). *Palaeopelagos* 6,
825 347-360.
- 826 Marsico, A., Selleri, A., Mastronuzzi, G., Sansò, P., Walsh, N., 2003. Cryptokarst: a
827 case-study of the Quaternary landforms of southern Apulia (southern Italy). *Acta*
828 *Carsologica* 32 (2), 147-159.
- 829 Mastronuzzi, G., Sansò, P., 1998. Morfologia e genesi delle Isole Chéradi e del Mar
830 Grande (Taranto, Puglia, Italia). *Geografia Fisica e Dinamica Quaternaria* 21,
831 131-138.
- 832 Mastronuzzi, G., Sansò, P., 2000. Boulders transport by catastrophic waves along the
833 Ionian coast of Apulia (southern Italy). *Marine Geology* 170, 93-103.
- 834 Mastronuzzi, G., Sansò, P., 2002a. Holocene uplift rates and historical rapid sea-level
835 changes at the Gargano promontory, Italy. *Journal of Quaternary Science* 17 (5-6),
836 593-606.
- 837 Mastronuzzi, G., Sansò, P., 2002b. Holocene coastal dune development and
838 environmental changes in Apulia (Southern Italy). *Sedimentary Geology* 150,
839 139-152.

- 840 Mastronuzzi, G., Sansò, P., 2002c. Pleistocene sea level changes, sapping processes and
841 development of valleys network in Apulia region (southern Italy).
842 *Geomorphology* 46, 19-34.
- 843 Mastronuzzi, G., Sansò, P., 2004. Large boulder accumulation by extreme waves along
844 the Adriatic coast of southern Apulia (Italy). *Quaternary International* 120, 173-
845 184.
- 846 Mastronuzzi, G., Pignatelli, C., Sansò, P., Selleri, G., 2007a. Boulder accumulations
847 produced by the 20th February 1743 tsunami along the coast of southeastern
848 Salento (Apulia region, Italy). *Marine Geology* 242 (1-3), 191-205,
849 doi:10.1016/j.margeo.2006.10.025.
- 850 Mastronuzzi, G., Quinif, Y., Sansò, P., Selleri, G., 2007b. Middle-Late Pleistocene
851 polycyclic evolution of a geologically stable coastal area (southern Apulia, Italy).
852 *Geomorphology* 86, 393-408.
- 853 Mazzoli, S., Helman M., 1994, Neogene patterns of relative plate motion for Africa–
854 Europe: Some implications for recent central Mediterranean tectonics.
855 *Geologische Rundschau* 83, 464-468.
- 856 Menardi Noguera, A., Rea, G., 2000. Deep structure of the Campanian-Lucanian Arc
857 (southern Apennines). *Tectonophysics* 324, 239-265.
- 858 Montone, P., Mariucci, M.T., Pondrelli, S., Amato, A., 2004. An improved stress map
859 for Italy and surrounding regions (central Mediterranean). *Journal of Geophysical*
860 *Research* 109, B10410, 1-22, doi: 10.1029/1003JB002703.
- 861 Moretti, M., 2000. Soft-sediment deformation structures interpreted as seismites in
862 middle-late Pleistocene aeolian deposits (Apulian foreland, Southern Italy).
863 *Sedimentology* 135, 167-179.
- 864 Moretti, M., Tropeano, M., 1996. Strutture sedimentarie deformative (sismiti) nei
865 depositi tirreniani di Bari. *Memorie della Società Geologica Italiana* 51, 485-500.
- 866 Mostardini, F., Merlini, S., 1986. Appennino centro-meridionale. Sezioni Geologiche e
867 Proposta di Modello Strutturale. *Memorie della Società Geologica Italiana* 35,
868 177-202.
- 869 Palmentola, G., 1987. Lineamenti geologici e morfologici del Salento leccese. Atti del
870 “Convegno sulle conoscenze geologiche del territorio salentino”. *Quaderni di*
871 *Ricerca del Centro Studi di Geotecnica e d’Ingegneria* 11, 173-202.
- 872 Papanikolaou, I.D., Roberts, G.P., 2007. Geometry, kinematics and deformation rates
873 along the active normal fault system in the southern Apennines: Implications for
874 fault growth. *Journal of Structural Geology* 29, 166-188.
- 875 Patacca, E., Scandone, P., 1989. Post-Tortonian mountain building in the Apennines.
876 The role of the passive sinking of a relic lithospheric slab. In: Boriani, A.M., et al.
877 (Eds.), *The Lithosphere in Italy*. *Atti dei Convegni Lincei* 80, 157-176.
- 878 Patacca, E., Scandone, P., 2004. The Plio-Pleistocene thrust belt – foredeep system in
879 the Southern Apennines and Sicily (Italy). In: Crescenti, U., et al. (Eds.), *Geology*
880 *of Italy*. *Società Geologica Italiana*, Roma, 93-129.
- 881 Piccardi, L., 2005. Paleoseismic evidence of legendary earthquakes: the apparition of
882 Archangel Michael at Monte Sant’Angelo (Italy). *Tectonophysics* 408, 113-128.

- 883 Pieri, P., Sabato, L., Tropeano, M., 1996. Significato Geodinamico dei caratteri
884 deposizionali e strutturali della Fossa Bradanica nel Pleistocene. Memorie della
885 Società Geologica Italiana 51, 501-515.
- 886 Pollard, D.D., Aydin, A., 1988. Progress in understanding jointing over the past century.
887 Bulletin of the Geological Society of America 100, 1181-1204.
- 888 Reches, Z., 1987. Determination of the tectonic stress tensor from slip along faults that
889 obey the Coulomb yield condition. Tectonophysics 6 (6), 849-861.
- 890 Ricchetti, G., 1967. Osservazioni preliminari sulla geologia e morfologia dei depositi
891 quaternari nei dintorni del Mar Piccolo (Taranto). Atti Accademia Gioenia
892 Scienze Naturali in Catania 6 (18), 123-130.
- 893 Ricchetti, G., 1972. Osservazioni geologiche e morfologiche preliminari sui depositi
894 quaternari affioranti nel F. 203 (Brindisi). Bollettino della Società dei Naturalisti
895 in Napoli 81, 543-566.
- 896 Ricchetti, G., 1980. Contributo alla conoscenza strutturale della Fossa Bradanica e delle
897 Murge. Bollettino della Società Geologica Italiana 99, 421-430.
- 898 Ridente, D., Trincardi, F., 2006. Active foreland deformation evidenced by shallow
899 folds and faults affecting late Quaternary shelf-slope deposits (Adriatic Sea, Italy).
900 Basin Research 18 (2), 171-188. doi: 10.1111/j.1365-2117.2006.00289.x
- 901 Ridente, D., Fracassi, U., Di Bucci, D., Trincardi, F., Valensise, G., 2008. Middle
902 Pleistocene to Holocene activity of the Gondola Fault Zone (Southern Adriatic
903 Foreland): deformation of a regional shear zone and seismotectonic implications.
904 In: Caputo, R., Pavlides, S. (Eds.), Earthquake Geology: methods and
905 applications. Tectonophysics 453 (1-4), 110-121. doi:10.1016/j.tecto.2007.05.009
- 906 Salvatorini, G., 1969. Contributo alla conoscenza delle microfaune pleistoceniche della
907 penisola salentina. Atti della Società Toscana di Scienze Naturali 76 (1), 232-260.
- 908 Serpelloni, E., Vannucci, G., Pondrelli, S., Argnani, A., Casula, G., Anzidei, M., Baldi,
909 P., Gasperini, P., 2007. Kinematics of the Western Africa-Eurasia plate boundary
910 from focal mechanisms and GPS data. Geophysical Journal International (Online-
911 Early Articles). doi:10.1111/j.1365-246X.2007.03367.x
- 912 Servizio Geologico d'Italia, 1967. Carta Geologica d'Italia, Fogli: 202 Taranto, 203
913 Brindisi, 204 Lecce, 213 Maruggio, 214 Gallipoli, 215 Otranto, 223 Capo S.
914 Maria di Leuca, 1:100.000. Servizio Geologico d'Italia, Roma.
- 915 Tinti, S., Maramai, A., Graziani, L., 2004. The new catalogue of Italian tsunamis.
916 Natural Hazards 33, 439-465.
- 917 Tropeano, M., Pieri, P., Moretti, M., Festa, V., Calcagnile, G., Del Gaudio, V., Pierri, P.
918 1997. Tettonica quaternaria ed elementi di sismotettonica nell'area delle Murge
919 (Avampaese Apulo). Il Quaternario 10 (2), 543-548.
- 920 Tropeano, M., Sabato, L., Pieri, P., 2002. Filling and cannibalization of a foredeep: the
921 Bradanic Trough (Southern Italy). In: Jones, S.J., Frostick, L.E. (Eds.), Sediment
922 flux to basins: causes, controls and consequences. Geological Society of London
923 Sp. Publ. 191, 55-79.
- 924 Tropeano, M., Spalluto, L., Moretti, M., Pieri, P., Sabato, L., 2004. Depositi carbonatici
925 infrapleistocenici di tipo Foramol in sistemi di scarpata (Salento, Italia)

- 926 Meridionale). *Il Quaternario, Italian Journal of Quaternary Sciences* 17 (2-2), 537-
927 546.
- 928 Valensise, G., Pantosti, D., Basili, R., 2004. Seismology and Tectonic Setting of the
929 Molise Earthquake Sequence of October 31-November 1, 2002. *Earthquake*
930 *Spectra* 20, 23-37.
- 931 Vannucci, G., Gasperini, P., 2004. The new release of the database of Earthquake
932 Mechanisms of the Mediterranean Area (EMMA Version 2). *Annals of*
933 *Geophysics Suppl.* 47, 307-334.
- 934

935 **Figure captions**

936

937 **Fig. 1.**

938 Geological sketch map of Southern Italy (Calabrian arc excluded). The Molise-Gondola
939 shear zone (MGsz) is also shown.

940

941 **Fig. 2.**

942 Historical and instrumental earthquakes of the Central and Southern Apennines ($M > 4.0$;
943 Gruppo di lavoro CPTI, 2004; Vannucci and Gasperini, 2004; Harvard CMT Project,
944 2006; Fracassi and Valensise, 2007). The size of the square symbols is proportional to
945 an equivalent magnitude derived from intensity data. The black thick line is the outer
946 front of the Southern Apennines buried below the foredeep deposits.

947

948 **Fig. 3.**

949 Geological sketch of the Salento Peninsula (redrawn, data from sources mentioned in
950 the legend). The Apulia carbonate platform (of Cretaceous-Paleocene age) crops out
951 primarily in the topographic highs to the N and NW (the Murge Plateau) and toward the
952 SE sector of Salento. Lower to Upper Pleistocene deposits are exposed in the Brindisi
953 Plain, along the coast from Porto Cesareo to Taranto and S of Gallipoli. Pleistocene to
954 Holocene deposits can be found only in few localities, mostly on the western sector of
955 the studied area but for the Otranto surroundings. Pl-Ho: Pleistocene-Holocene
956 alluvium; MUPl: Middle-Upper Pleistocene terraced coastal plain and limestone
957 breccias; MiPl: Middle Pleistocene sands (Sabbie di Montemarano Fm); LoPl: Lower
958 Pleistocene shales and marls (Argille subappennine Fm) and calcarenites and littoral
959 calcirudites (Calcareniti di Gravina Fm); K-LT: Lower Tertiary open shelf carbonates
960 (Pietra Leccese and Calcareniti di Andrano Fms) and Cretaceous platform limestone
961 (Calcareniti di Bari and Calcareniti di Altamura Fms). Simplified from Ciaranfi et al. (1988).

962

963 **Fig. 4.**

964 Examples of analyzed deposits: **a)** cemented dune, Holocene, site Sal009 (Lon. E
965 17.701, Lat. N 40.760), **b)** marine calcarenites with *Strombus bubonius* Linnaeus, Upper
966 Pleistocene, site Sal033, **c)** Marine Terraced Deposits, Middle-Upper Pleistocene, site
967 Sal032; **d)** Gravina Fm marine calcarenites, late Lower Pleistocene, site Sal019.

968

969 **Fig. 5.**

970 Examples of analyzed joints: **a)** extension joints at the outcrop scale, site Sal021; **b)**
971 systematic joint set, site Sal069; **c)** orthogonal joint sets, site Sal011; **d)** two joints
972 chronologically distinguished, i.e., an older calcite-filled fracture cut by a younger
973 sedimentary vein, site Sal034.

974

975 **Fig. 6.**

976 Examples of analysis of the joint systems, where fractures are plotted as poles to the
977 planes in stereographic projections, lower hemisphere. The size of the symbols (crosses)
978 is proportional to the corresponding amount of opening and length of the joints. The
979 latter information has been included in the numerical inversions as a statistical weight.
980 Triangles, rhombi and squares represent the principal stress axes σ_1 , σ_2 and σ_3 ,
981 respectively. Referring to these axes, the upper triplets of numbers indicate azimuth and
982 plunge, while the lower ones represent the normalized weight from which the ratio R is
983 obtained. **a)** Single joint set. **b)** Two well developed, roughly orthogonal sets. **c)** and **d)**
984 More than two joint sets within the same site (black and gray crosses). In these latter
985 cases, data have been separated before applying the numerical inversion method
986 (Caputo and Caputo 1989). See text for further details.

987

988 **Fig. 7.**

989 Deformational events recognized. For each plot, the number on the top-right refers to
990 the site label (see also Tabs. 1 to 3). On the maps, the arrows in the large circles show
991 the direction of horizontal extension, while the gray-scale of the circles refers to the age
992 of the youngest deposit involved at the site (black = late Lower Pleistocene; gray =
993 Middle, late Middle and Middle-Upper Pleistocene; white = Upper Pleistocene). The
994 small white dots are all the investigated sites. **a)** First subset of data (see also Tab. 1),
995 that has been associated with the oldest deformational event recognized, ascribed to the
996 early and middle part of the Middle Pleistocene. **b)** Second subset of data (see also Tab.
997 2), that has been associated with the penultimate deformational event defined, ascribed
998 to the late Middle Pleistocene. **c)** Third subset of data (see also Tab. 3), that has been
999 associated with the most recent deformational event recognized, not older than the Late
1000 Pleistocene.

1001

1002

1003 **Fig. 8.**

1004 Summary of the deformational events defined. Each plot shows the principal axes
1005 grouped per event, and their mean values (larger symbols; angular deviation in
1006 parentheses). Events are referred to the: **a)** early and middle part of the Middle
1007 Pleistocene (site Sal034 omitted); **b)** late Middle Pleistocene; **c)** Late Pleistocene. See
1008 also Figures 7a-c and Tables 1-3.

1009

1010 **Fig. 9.**

1011 Geodynamic interpretation proposed in this work. Dashed lines are depth contours in
1012 kilometres of the subducting slab. A gray line marks the axis of the Apennine-
1013 Maghrebian chain, that is currently undergoing extension. The Africa plate relative
1014 motion, referred to the Europe fixed reference (thick black arrows), is from Devoti et al.
1015 (2008). Large gray arrows indicate the front motion of the schematised chains.

1016

1017

1018

1019

1020 **Table captions**

1021

1022 **Table 1.**

1023 First subset of data collected within the investigated area (see also Fig. 7a). Data refer to
1024 the oldest deformational event recognized, ascribed to the early and middle part of the
1025 Middle Pleistocene. The *age* is that of the youngest deposits involved at the site. The
1026 *relative age* indicates the occurrence of abutting relationships with a joint system
1027 associated with another deformational event. The latter subset of data is represented in
1028 the corresponding table only if a statistically meaningful numerical inversion has been
1029 performed. σ_1 , σ_2 and σ_3 are the principal stress axes (maximum, intermediate and
1030 minimum, respectively). R is the stress ratio: $(\sigma_2 - \sigma_3)/(\sigma_1 - \sigma_3)$.

1031

1032 **Table 2.**

1033 Second subset of data collected within the investigated area (see also Fig. 7b). Data
1034 refer to the penultimate deformational event recognized, ascribed to the late Middle
1035 Pleistocene. Explanations as in Table 1.

1036

1037 **Table 3.**

1038 Third subset of data collected within the investigated area (see also Fig. 7c). Data refer
1039 to the most recent deformational event recognized, not older than the Late Pleistocene.

1040 Explanations as in Table 1.

1041

1042

1043 **Table 1.** First subset of data.

<i>label</i>	<i>long.</i> (°E)	<i>lat.</i> (°N)	<i>location</i>	<i>lithology / formation</i>	<i>age</i>	<i>relative age</i>	<i># of data</i>	σ_1 azim/dip	σ_2 azim/dip	σ_3 azim/dip	<i>R</i>
Sal012	17.192	41.012	Torre Incina	Marine calcarenite (Gravina Fm)	late Early Pleistocene	older than subset 2	54	119/88	282/02	012/01	0.87
Sal034	18.449	40.029	Torre di Porto Miggiano	Marine calcarenite (Gravina Fm)	late Early Pleistocene	possibly older than subset 1	105	146/83	001/06	271/04	0.98
Sal061	17.739	40.341	Avetrana quarry	Marine calcarenite (Gravina Fm)	late Early Pleistocene		66	285/85	098/05	188/01	0.99
Sal063	18.394	39.861	Novaglie	Marine calcarenite (Gravina Fm)	late Early Pleistocene		74	046/86	267/03	177/03	0.64
Sal064	18.137	40.334	Lecce by-pass road (Monteroni)	Marine calcarenite (Gravina Fm)	late Early Pleistocene	older than subset 2	134	090/88	282/02	192/00	0.97
Sal067	17.669	40.477	Oria quarry	Marine calcarenite (Gravina Fm)	late Early Pleistocene		101	102/41	276/49	009/03	0.99

1044

1045

1046 **Table 2.** *Second subset of data.*

1047

<i>label</i>	<i>long.</i> (°E)	<i>lat.</i> (°N)	<i>location</i>	<i>lithology / formation</i>	<i>age</i>	<i>relative age</i>	<i># of data</i>	σ_1 <i>azim/dip</i>	σ_2 <i>azim/dip</i>	σ_3 <i>azim/dip</i>	<i>R</i>
Sal012	17.192	41.012	Torre Incina	Marine calcarenite (Gravina Fm)	late Early Pleistocene	older than subset 3	33	348/82	151/08	242/02	0.98
Sal022	18.122	40.498	Casalabate, Intendenza di Finanza	Marine calcarenite with quartz	Middle Pleistocene		30	145/89	303/01	033/00	0.90
Sal032	18.027	40.057	Gallipoli. S. Maria delle Grazie quarry	Terraced marine calcarenite	late Middle Pleistocene	younger than subset 1	20	129/82	322/07	232/02	0.91
Sal064	18.137	40.334	Lecce by-pass road (Monteroni)	Marine calcarenite (Gravina Fm)	late Early Pleistocene	older than subset 3	21	134/28	329/62	227/06	0.99
Sal065	17.794	40.441	W of San Pancrazio Salentino	Marine calcarenite (Gravina Fm)	late Early Pleistocene		22	084/84	321/03	231/05	0.99
Sal066	17.807	40.453	S. Antonio	Marine calcarenite (Gravina Fm)	late Early Pleistocene		36	038/89	131/00	221/01	0.95
Sal069	18.044	40.156	Castellino, quarry between Nardò and Galatone	Marine calcarenite (Gravina Fm)	late Early Pleistocene		151	148/21	330/69	238/01	0.99
Sal070	18.103	40.073	Tuglie quarry	Marine calcarenite (Gravina Fm)	late Early Pleistocene		25	274/87	112/03	022/01	0.85
Sal072	18.115	40.506	Torre Specchiolla, N of Casalabate	Terraced marine deposits, clinostratified	Middle-Late Pleistocene	younger than subset 1	53	336/90	122/00	212/00	0.90
Sal077	17.912	40.267	Porto Cesareo, Crossroad Nardò-Avetrana	Marine calcarenite (Gravina Fm)	late Early Pleistocene		103	044/87	307/00	217/03	0.86

1048

1049 **Table 3.** Third subset of data.

1050

label	long. (°E)	lat. (°N)	location	lithology / formation	age	relative age	# of data	σ_1 azim/dip	σ_2 azim/dip	σ_3 azim/dip	R
Sal011	17.192	41.015	S. Vito Abbey	Marine calcarene (Gravina Fm)	late Early Pleistocene		115	255/89	072/01	162/00	0.20
Sal021	17.936	40.683	Punta Penne	Clinostratified calcarene, split (drift NW to SE)	Late Pleistocene?		74	314/87	182/02	092/02	0.22
Sal032	18.027	40.057	Gallipoli. S. Maria delle Grazie quarry	Terraced marine calcarene	late Middle Pleistocene	younger than subset 2	31	121/87	287/03	017/01	0.47
Sal033	17.993	40.061	Gallipoli coast	Marine calcarene with <i>Strombus bubonius</i>	Late Pleistocene		25	253/88	029/02	119/02	0.42
Sal034	18.449	40.029	Torre di Porto Miggiano	Marine calcarene (Gravina Fm)	late Early Pleistocene	younger than subset 1	57	085/86	178/00	268/04	0.14
Sal059	17.642	40.776	Costa Merlata	Marine calcarene (Gravina Fm)	late Early Pleistocene		61	207/89	031/00	301/00	0.30
Sal062	18.408	39.976	Andrano, Grottaverde	Marine calcarene (Gravina Fm)	late Early Pleistocene		32	276/88	099/02	009/00	0.16
Sal071	18.112	40.494	Quarry near Casalabate	Terraced marine deposits	Middle-Late Pleistocene		51	086/88	298/01	208/01	0.47
Sal072	18.115	40.506	Torre Specchiolla, N of Casalabate	Terraced marine deposits; clinostratified	Middle-Late Pleistocene	younger than subset 2	42	162/89	351/01	261/00	0.47
Sal074- Sal075	18.093	39.897	N of Torre S. Giovanni and Isola dei Pazzi	Dune with foresets and bioturbations Dune overlying marine calcarene rich in algae	Late Pleistocene		24	137/88	029/01	299/02	0.17
Sal076	18.111	39.886	S of Torre S. Giovanni	Marine calcarene rich in algae	Late Pleistocene		54	013/89	171/00	261/00	0.04
Sal078	17.358	40.354	Lido Silvana, Pulsano	Calcarene	Late Pleistocene		26	034/83	278/03	187/06	0.45

1051

Figure 1

[Click here to download high resolution image](#)

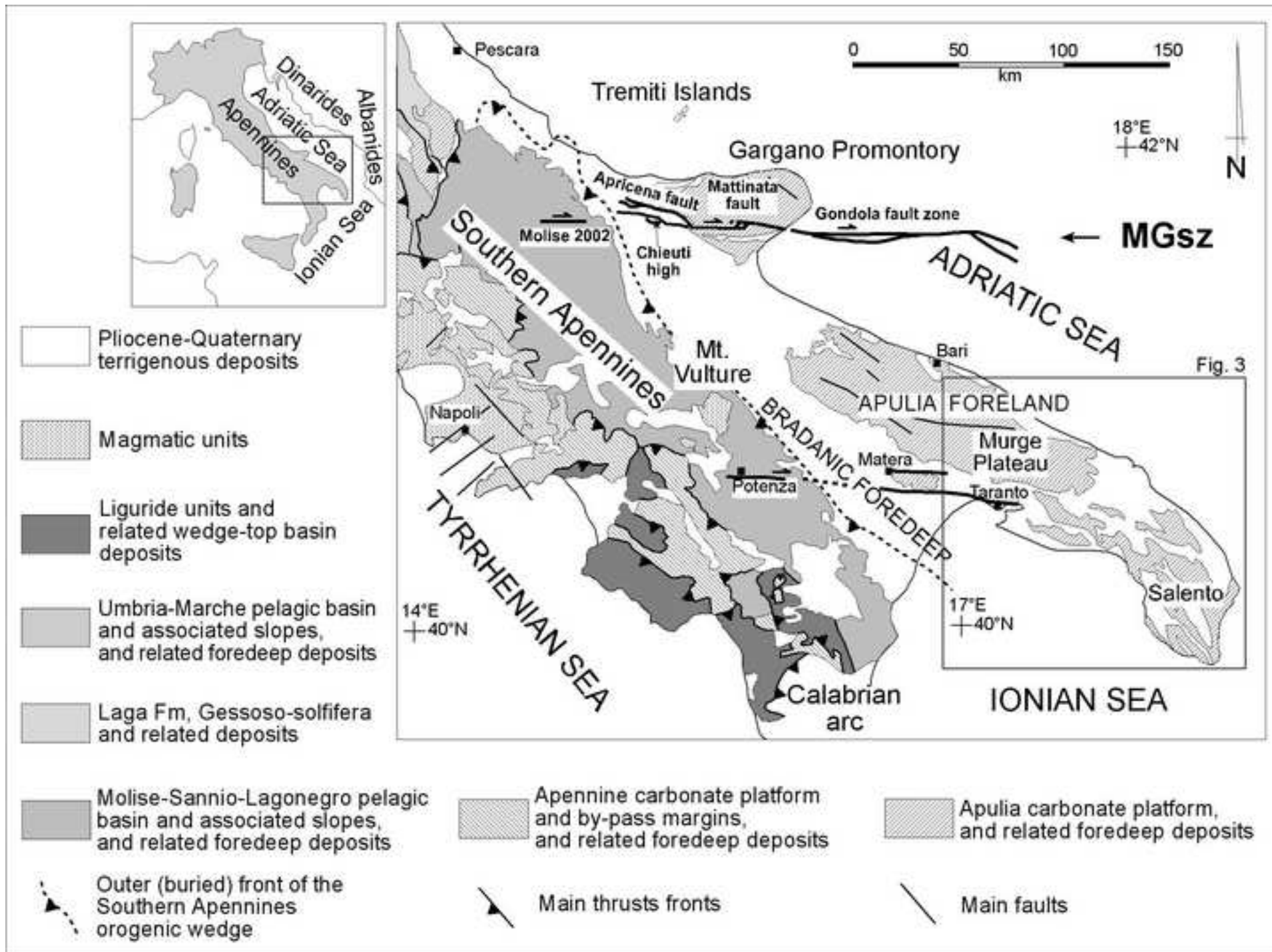


Figure 2
[Click here to download high resolution image](#)

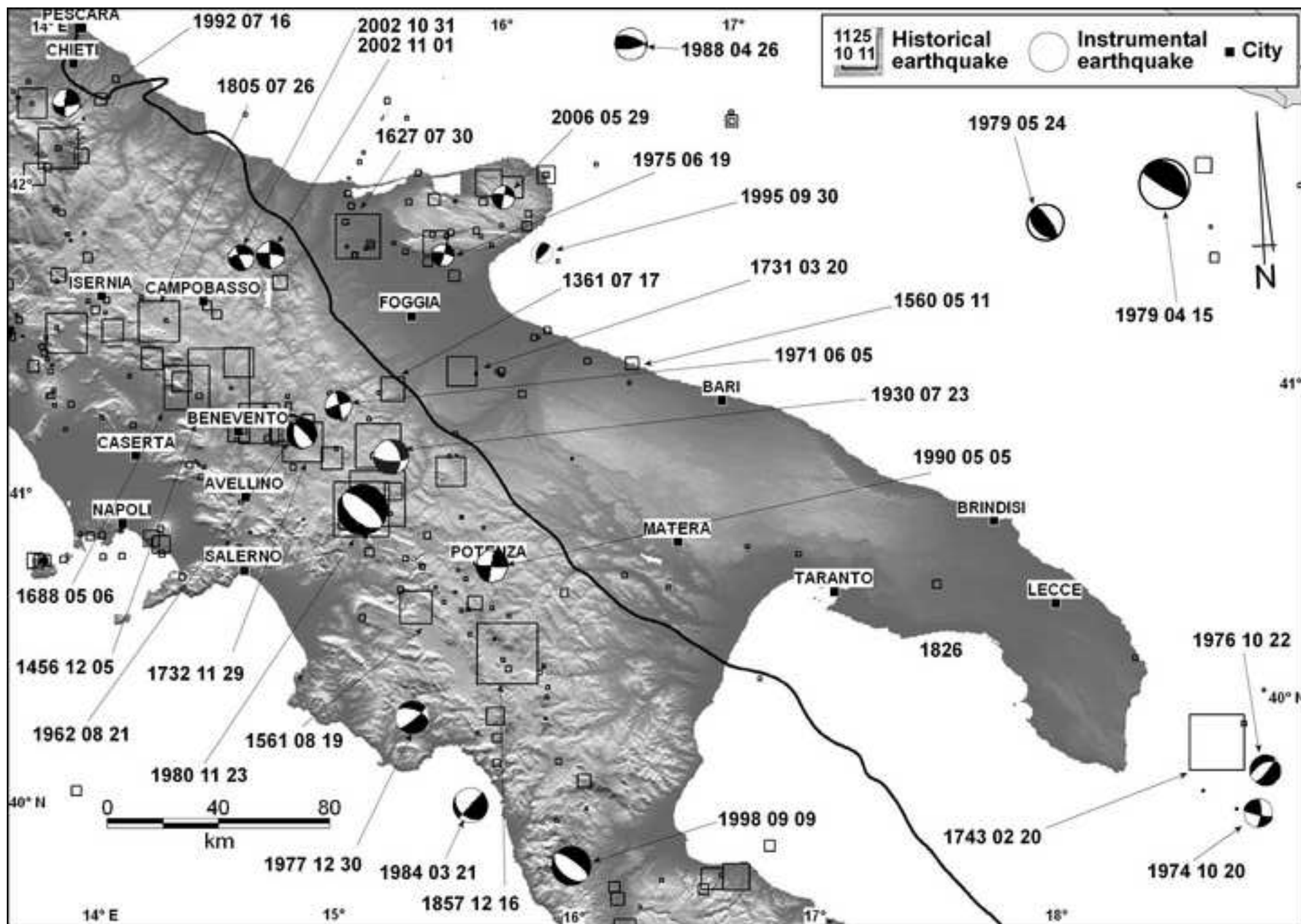


Figure 3
[Click here to download high resolution image](#)

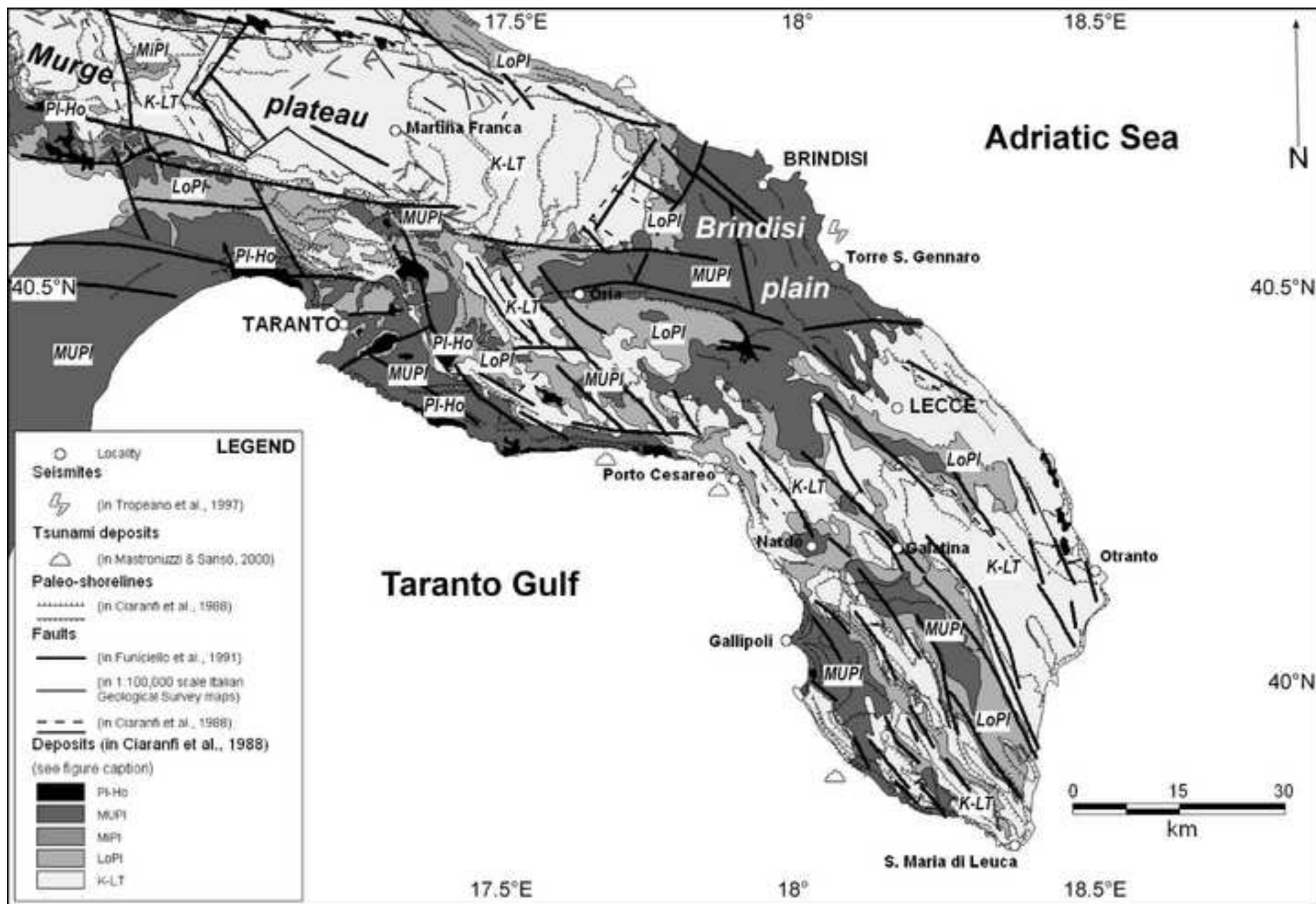


Figure 4
[Click here to download high resolution image](#)

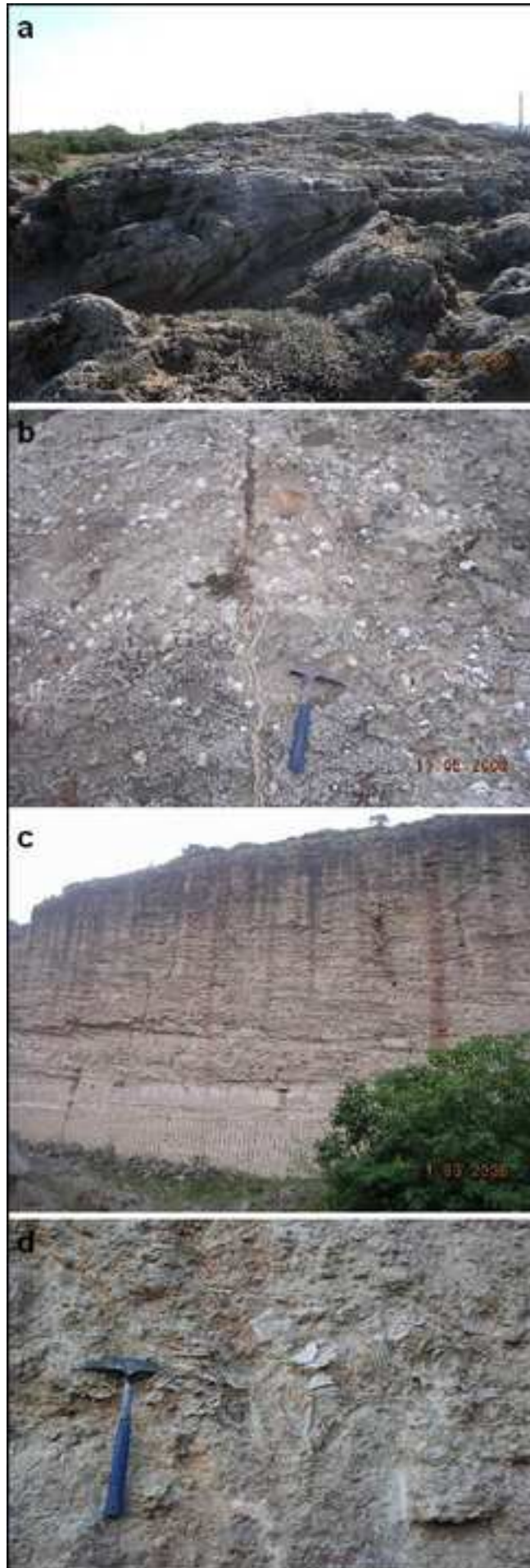


Figure 5
[Click here to download high resolution image](#)

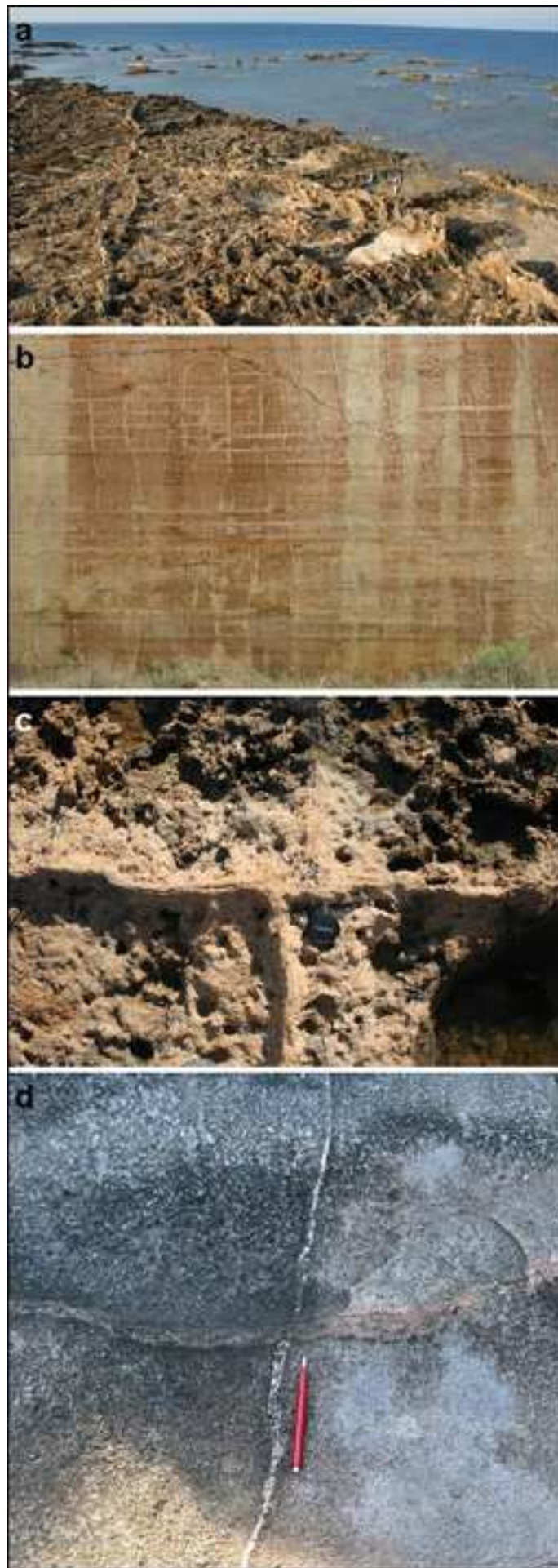


Figure 6
[Click here to download high resolution image](#)

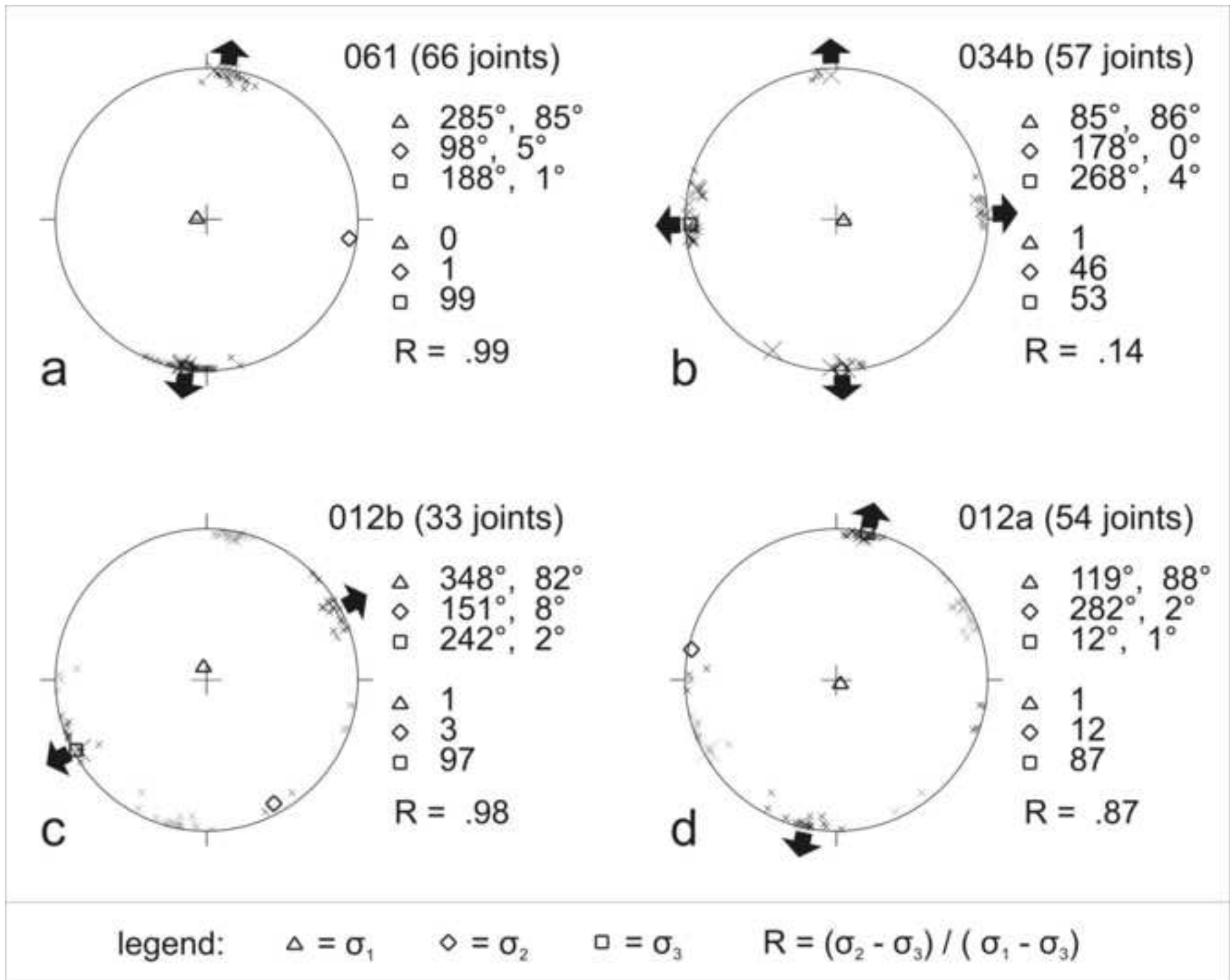


Figure 7a
[Click here to download high resolution image](#)

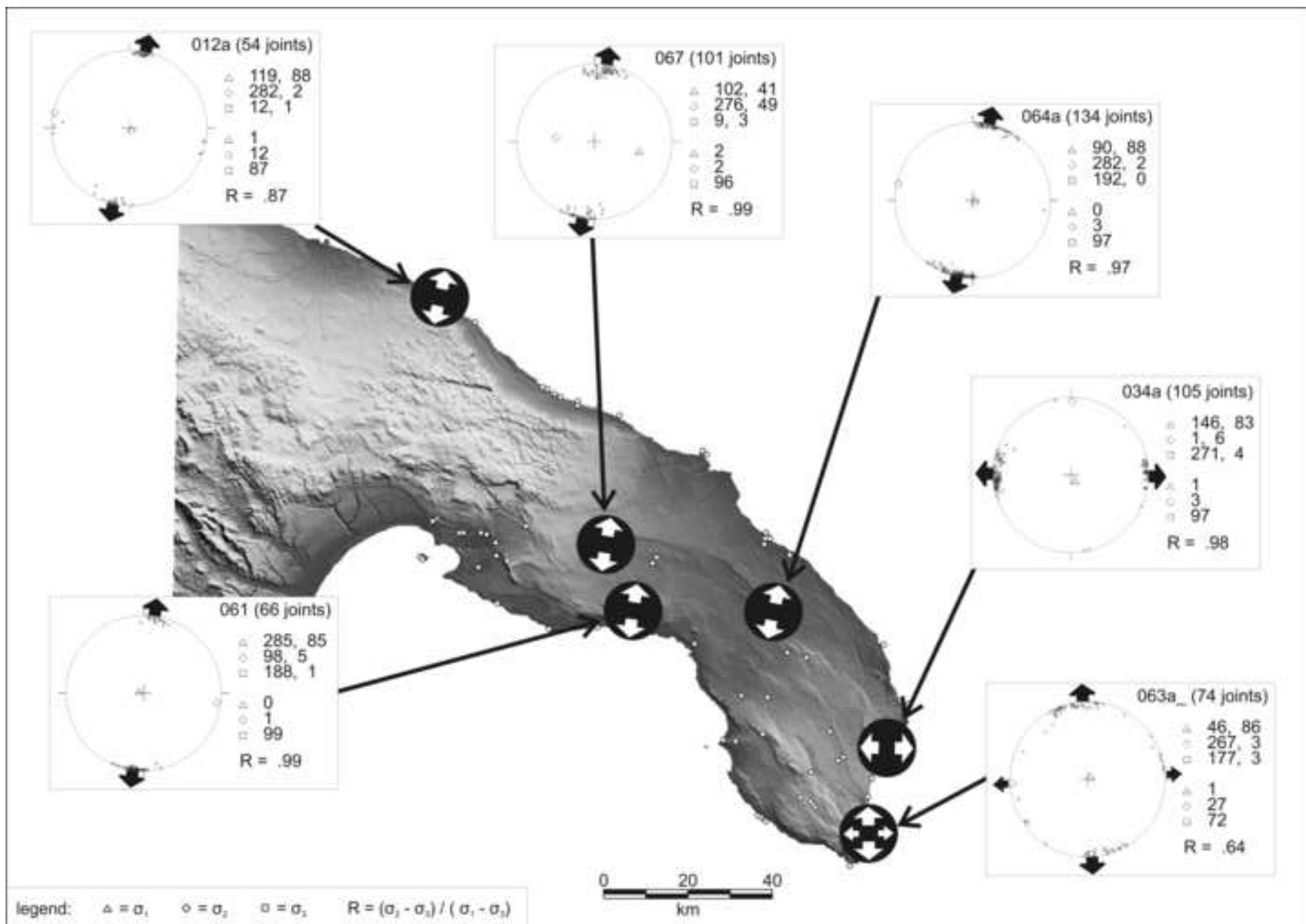


Figure 7b
[Click here to download high resolution image](#)

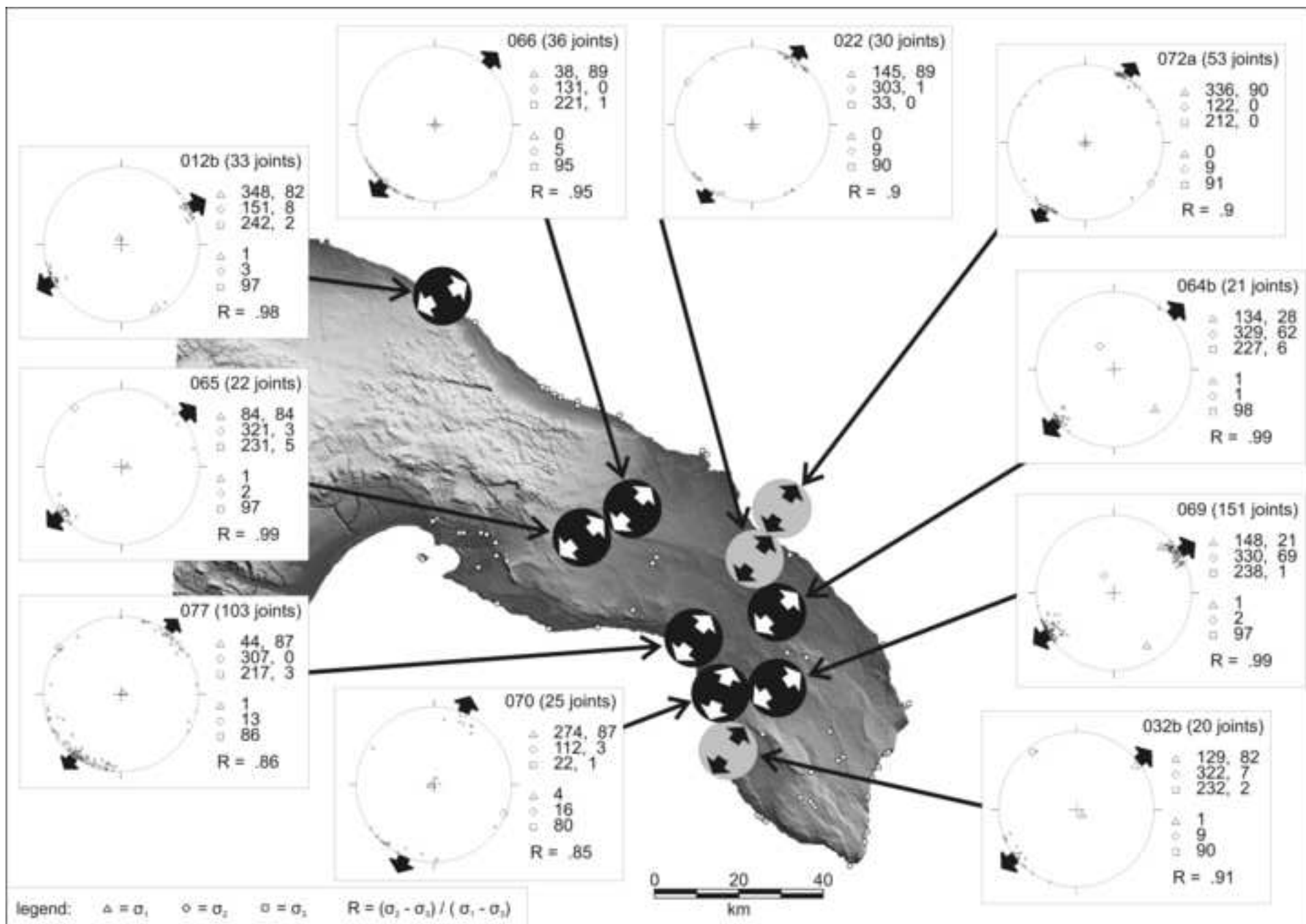


Figure 7c
[Click here to download high resolution image](#)

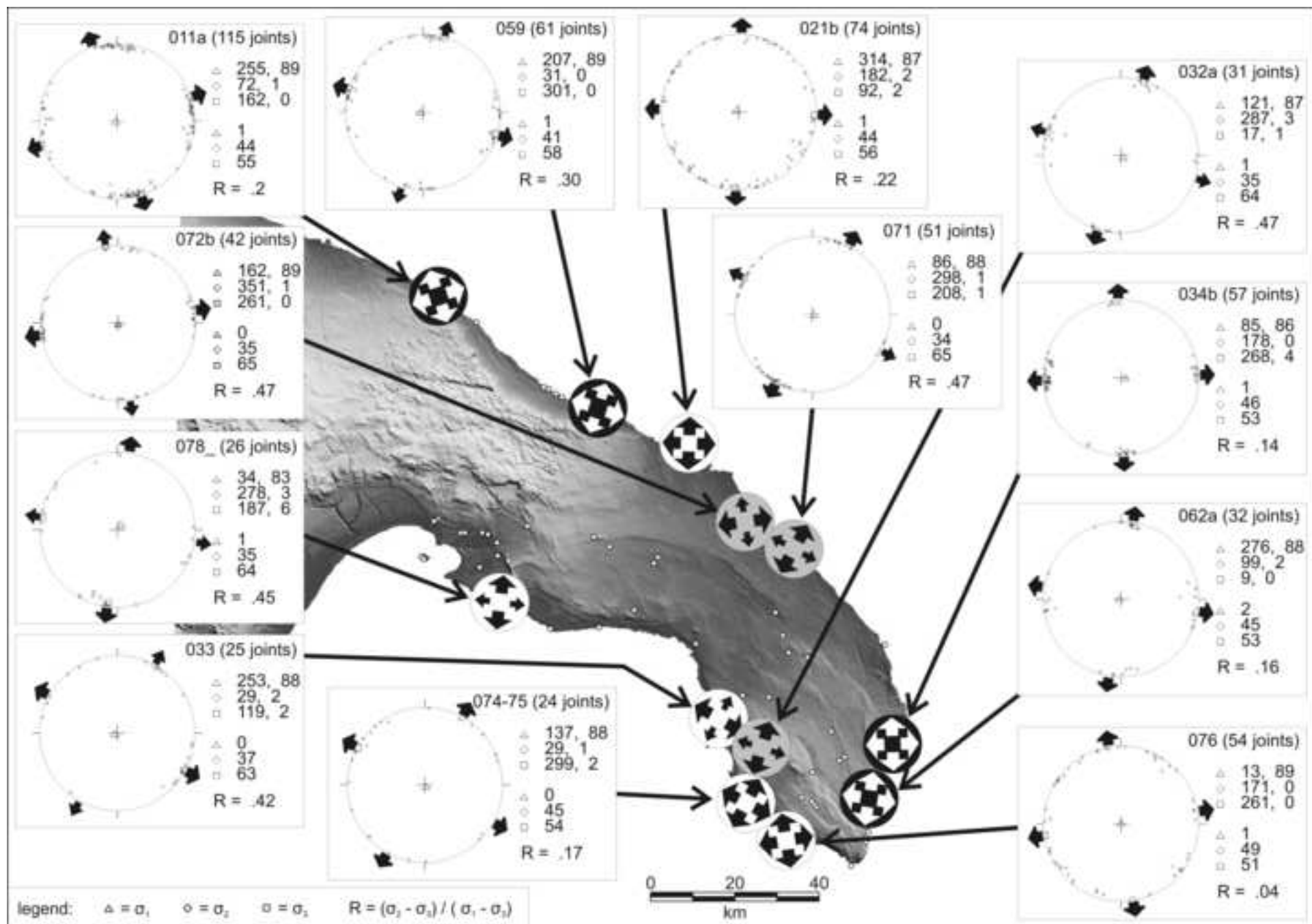


Figure 8

[Click here to download high resolution image](#)

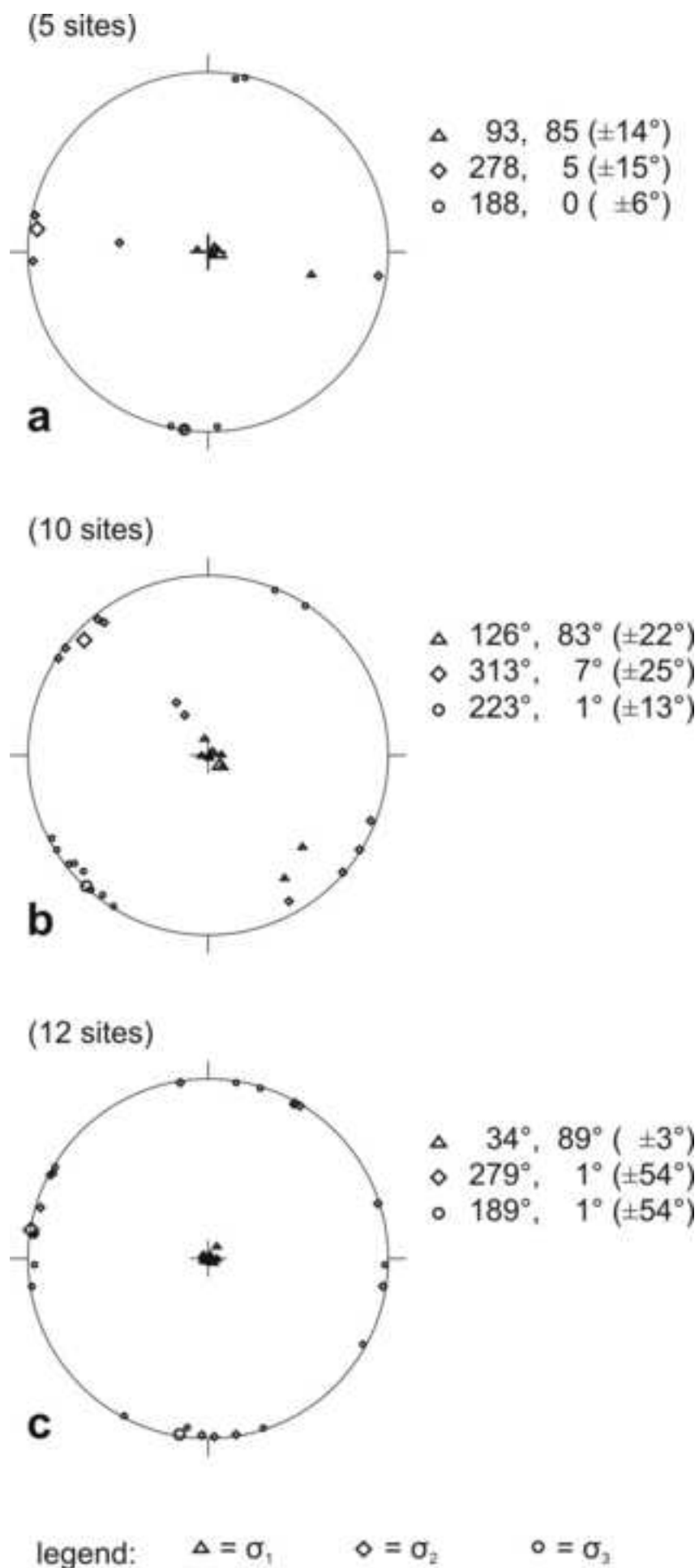


Figure 9

[Click here to download high resolution image](#)

